Journal of Controlled Release 332 (2021) 40–63

Contents lists available at ScienceDirect

Journal of Controlled Release

journal homepage: www.elsevier.com/locate/jconrel

Review article

Aerogels in drug delivery: From design to application

Carlos A. García-González [a], Alejandro Sosnik [b], József Kalmár [c], Iolanda De Marco [d], Can Erkey [e], Angel Concheiro [a], Carmen Alvarez-Lorenzo [a,*]

[a] Departamento de Farmacología, Farmacia y Tecnología Farmacéutica, I+D Farma (GI-1645), Facultad de Farmacia and Health Research Institute of Santiago de Compostela (IDIS), Universidade de Santiago de Compostela, 15782 Santiago de Compostela, Spain
[b] Laboratory of Pharmaceutical Nanomaterials Science, Department of Materials Science and Engineering, Technion-Israel Institute of Technology, Haifa, Israel
[c] Department of Inorganic and Analytical Chemistry, University of Debrecen, Egyetem tér 1, Debrecen H-4032, Hungary
[d] Department of Industrial Engineering, University of Salerno, Via Giovanni Paolo II, 132, 84084 Fisciano, SA, Italy
[e] Chemical and Biological Engineering Department, Koç University, 34450 Sarıyer, Istanbul, Turkey

ARTICLE INFO

Keywords:
Aerogel
Dissolution enhancer
Controlled release
Stimuli-responsive
Oral administration
Lung
3D printing
Supercritical fluid
Theranostic
Life cycle assessment

ABSTRACT

Aerogels are the lightest processed solid materials on Earth and with the largest empty volume fraction in their structure. Composition versatility, modularity, and feasibility of industrial scale manufacturing are behind the fast emergence of aerogels in the drug delivery field. Compared to other 3D materials, the high porosity (interconnected mesopores) and high specific surface area of aerogels may allow faster loading of small-molecule drugs, less constrained access to inner regions of the matrix, and more efficient interactions of the biological milieu with the polymer matrix. Processing in supercritical CO_2 medium for both aerogel production (drying) and drug loading (impregnation) has remarkable advantages such as absence of an oxidizing environment, clean manufacture, and easiness for the scale-up under good manufacturing practices. The aerogel solid skeleton dictates the chemical affinity to the different drugs, which in turn determines the loading efficiency and the release pattern. Aerogels can be used to increase the solubility of BCS Class II and IV drugs because the drug can be deposited in amorphous state onto the large surface area of the skeleton, which facilitates a rapid contact with the body fluids, dissolution, and release. Conversely, tuning the aerogel structure by functionalization with drug-binding moieties or stimuli-responsive components, application of coatings and incorporation of drug-loaded aerogels into other matrices may enable site-specific, stimuli-responsive, or prolonged drug release. The present review deals with last decade advances in aerogels for drug delivery. An special focus is paid first on the loading efficiency of active ingredients and release kinetics under biorelevant conditions. Subsequent sections deal with aerogels intended to address specific therapeutic demands. In addition to oral delivery, the physical properties of the aerogels appear to be very advantageous for mucosal administration routes, such as pulmonary, nasal, or transdermal. A specific section devoted to recent achievements in gene therapy and theranostics is also included. In the last section, scale up strategies and life cycle assessment are comprehensively addressed.

1. Introduction

Processing of advanced materials as aerogels has opened new ways of addressing a variety of technological challenges while fulfilling eco-friendly criteria. Aerogels are mainly featured by their physical structure: solid with extremely low density (0.0001 to 0.2 g/cm^3), porosity larger than 90% with predominance of open pores in the mesoscale (2–50 nm), and high specific surface area (>200 m^2/g) [1,2]. Therefore, aerogels are the lightest processed solid materials on Earth with the largest empty volume fraction in their structure. Empty space filled with air or other gases notably contributes, for example, to the outstanding insulation capability of aerogel materials, offering novel strategies to achieve requirements of low weight and minimal waste of space of modern energy storage and transfer in industrial installations, buildings, and transport vehicles [3]. Aerogels also show outstanding capabilities for sorption of metals, solvents, fuel and oil spills as well as gases, being useful in selective captures for catalysis and analytical purposes and remediation [4–6]. In parallel, the versatility of the materials that can be used (e.g., ceramics, metals, polymers and hybrids), the mild conditions required for processing, and the variety of obtainable shapes are very

* Corresponding author.
E-mail address: carmen.alvarez.lorenzo@usc.es (C. Alvarez-Lorenzo).

https://doi.org/10.1016/j.jconrel.2021.02.012
Received 22 December 2020; Received in revised form 5 February 2021; Accepted 6 February 2021
Available online 16 February 2021
0168-3659/© 2021 The Author(s). Published by Elsevier B.V. This is an open access article under the CC BY license (http://creativecommons.org/licenses/by/4.0/).

appealing to explore applications in the biomedical field [7,8]. In addition, the use of advanced fabrication methods such as additive manufacturing in the processing of aerogels enhances their favorable properties even more [9,10]. Silica-based aerogels are the most widely investigated aerogels, but the field of biopolymer (polysaccharide, protein, nucleic acid) aerogels is rapidly growing for both biomedical and non-biomedical applications demanding improved mechanical properties, sustainability, biocompatibility and biodegradability [11–13].

By definition, an aerogel is generated by the replacement of the liquid inside a gel with a gas [14]. Similar to the hydrogels widely used in biomedicine, aerogels are also formed by 3D networks of organic polymers, inorganic materials or composites assembled colloidal materials. The main difference relies in the extraordinary greater degree of swelling of the dried network of aerogels. Such an expanded structure is made permanent by stretching the chains or the self-assembled components to levels that are hardly obtained yet by immersion in common solvents followed by conventional solvent evaporation techniques. Freeze-drying is intended to keep the original swelling achieved by the hydrogel in a favorable aqueous medium through rapid freezing of water inside the pores followed by sublimation under low pressure conditions. Nevertheless, the liquid-gas surface tension and liquid-solid adhesive forces may lead to the shrinking of the pores and promote further solid-solid interactions. Expansion of water during freezing may also damage the structure. Cosolvents that reduce surface tension (e.g., tert-butyl alcohol) or the use of cryoprotectants (e.g. trehalose combined with polyethylene glycol, PEG) can attenuate some of these drawbacks [15]. Differently, production of aerogels applying supercritical processing involves several changes of the liquid phase with organic solvents and subsequent extraction/drying under supercritical conditions (commonly in the presence of supercritical CO_2; $scCO_2$). This processing avoids the liquid-gas surface tension and liquid-solid adhesive forces and, therefore, prevents the collapse of the original pores [16]. The supercritical drying technology is compatible with a variety of solvents and even enables the use of poorly-water soluble materials that are not suitable as hydrogel components. Detailed comparative analysis of freeze-drying and supercritical drying processes and their respective outcomes can be found in recent reports [2,11]. The advent of non-supercritical drying techniques may further expand the aerogels field in a near future.

A priori, homogeneous structure, tunable mesh size, interconnected pores, and increased surface area appear as advantageous features for exploring the capabilities of aerogels as drug delivery systems. Compared to common pharmaceutical hydrogels and their freeze-dried spongy cryogels, aerogels may allow faster loading of small-molecules, less constrained access to inner regions of the matrix, and more efficient interactions with the polymer matrix. The aerogel solid skeleton dictates the chemical affinity of the matrix to the adsorbed molecule and, in the case of drugs, their partition coefficient between the aerogel and the aqueous medium when immersed in body fluids. However, some concerns on the use of aerogels as drug delivery platforms may also raise. The predominance of mesopores and the absence of larger pores in conventional aerogels may result in size exclusion effects that hinder the uptake of bulky molecules and therapeutic macromolecules in the aerogel network, compared to sponges or particles endowed with hierarchical porosity [17]. Moreover, wetting in aqueous fluids may trigger the collapse of the forcedly stretched chains to a more thermodynamically stable conformation or even the dissolution if the chains are not chemically crosslinked. Therefore, drug loading into preformed aerogels is so far mostly carried out in $scCO_2$ medium (as explained in more detail in the next section). The critical point of CO_2 (31.1 °C, 7.4 MPa) is compatible with the stability range of most drugs and proteins. Drug solubility in $scCO_2$ can be enhanced either by increasing the pressure or by adding cosolvents and, after processing, CO_2 evaporates and no traces of solvent remain in the aerogel. The absence of oxygen, the feasibility of carrying out the drug loading under clean conditions, and the easiness for the scale-up and production under good manufacturing practices (GMP) are remarkable advantages from the perspective of manufacturing of pharmaceutical grade products [18,19].

Another limitation is that once the drug-loaded aerogel is administered to the body, the large surface contact area with the physiological media may lead to fast and uncontrolled drug release, especially if the solubility and partition coefficient of the drug into the body fluids are high [11]. Nevertheless, regulation of the components solubility, degree of crosslinking, functionalization and interactions with the drug, as well as specific coatings and incorporation of aerogels in other matrices could be implemented to fine-tune the capability of aerogels to perform as platforms for controlled drug release or, oppositely, may further promote their role as fast dissolving solubility enhancers [20–23].

Some physical properties of the aerogels appear to be very advantageous for drug delivery through a variety of parenteral and, especially, mucosal administration routes [14]. The high capability of aerogels to absorb liquids may facilitate a precise regulation of the sorption of exudates from skin wounds and preserve moisture levels that promote wound healing, while the aerogel still regulates drug release [24]. Enhanced drug solubility and improved dissolution rate have been shown to promote drug penetration through the dermis [25], and therefore aerogels may be useful for transdermal treatments. Also, the low apparent density of aerogels makes them particularly appealing for pulmonary administration both for local treatment of lung diseases and for the systemic delivery (transpulmonary) of labile biopharmaceuticals, including those for gene therapy and vaccination [26–28]. Moreover, selective nasal administration may be feasible by regulating the particle size and adhesion properties [29].

Owing to their great versatility, modularity, and feasibility of manufacturing in an industrial scale, aerogels have emerged as one of the most exciting and promising platforms for drug delivery. In the last decade, there has been a growing interest in exploring the performances of aerogels in drug formulation as reflected in the increasing number of publications collected in the Web of Science database for the search criteria “aerogel AND drug delivery” (Fig. 1). There are also several other potential applications of aerogels in biomedicine, such as regenerative medicine, bioimaging and biosensors, which have been covered elsewhere [30–33].

This review deals with the peculiarities of aerogels as drug carriers and critically discusses their current and future contribution to the field of advanced drug delivery. Previous reviews on aerogels and drug delivery have mainly focused on the aerogel perspective and classified the information attending to the aerogel composition (inorganic/organic) and preparation protocols [34–36]. The field is evolving very rapidly (ca. 200 papers in the last 5 years), and recent reports have provided relevant information not only on characterization of textural properties

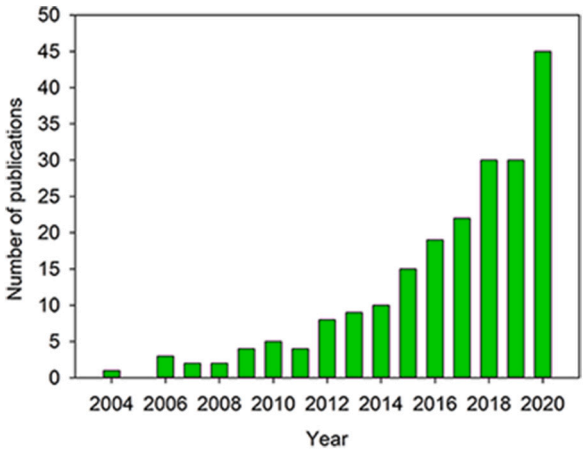


Fig. 1. Number of publications in Web of Science Core Collection database for the search criteria “aerogel AND drug delivery” (search date: December 18, 2020).

and drug loading and release tests in vitro, but also on in vivo proof-of-concepts for addressing specific therapeutic demands. Therefore, the present work firstly focuses in Section 2 on the advances made over last decade and that were devoted to understand how aerogels can fulfil the demands of drug formulations in terms of drug loading content, solubilization, physicochemical stability, and drug release kinetics and targeting. Following sections (Sections 3 to 5) gather the information from the perspective of feasible administration routes for drug-loaded aerogels to address specific therapeutic demands. Special focus is paid first on the loading efficiency of active ingredients and release kinetics under biorelevant conditions. Also, novel formats such as 3D printed aerogels and their potential are analyzed [10,26,37]. Finally, engineering-based scale up strategies and life cycle assessment are addressed in the last section of this review.

2. Drug loading into and release from aerogels: mechanisms and variables

2.1. Drug loading modalities and outcomes

Several protocols to integrate drugs during the fabrication process or once the aerogels are formed have been explored [38]. The four main strategies for the loading of drugs into aerogels (Fig. 2) are explained below.

(a) The first strategy, and apparently the simplest one, consists in adding the drug to the precursor solution of the gel (e.g., polymer dispersion). This approach uses drugs that are stable under the gelling conditions and poorly soluble both in the organic solvents used for solvent exchange and in the supercritical fluid used for drying to avoid premature drug extraction [35]. An excellent example is nicotinic acid; its solubility is 1.67 g/100 mL water, 0.7 g/100 mL ethanol and $1.84{\cdot}10^{-4}$ g/100 mL $scCO_2$ (35 °C, 100 bar). Therefore, alginate aerogels loaded with nicotinic acid can be prepared by adding the drug to the alginate aqueous solution before gel crosslinking, exchange of water with ethanol, and $scCO_2$ drying [39]. Interestingly, the presence of the drug notably attenuated the shrinkage of the alginate hydrogels in ethanol, favoring the production of aerogels with higher surface areas. Drugs that are soluble in water, organic solvents and $scCO_2$ may require processing by freeze-drying instead of $scCO_2$ drying [40] or by impregnation using supercritical fluids (as described below in strategy d).

(b) Alternatively, for drugs that are soluble in alcohols but not in $scCO_2$, the gel can be prepared first and then soaked into the drug solution for loading. Subsequent supercritical drying leads to drug precipitation inside the aerogel pores as the solvent is being removed [41]. This process resembles a gas antisolvent crystallization [32] and, differently to the other strategies, the outcome is the high loading of the drug in the crystalline state. Since the drug solubility in water is low, the release is mainly governed by drug dissolution and favored by the increased surface area provided by the aerogel matrix. However, the drug loading process could be slow (especially in the inner pores) and incomplete, as observed with silica aerogels exposed to paracetamol solutions. Drug diffusion from the outer concentrated medium to the inner pores of silica requires quite a long time. Therefore, in the typical timeframe of the preparation protocol, a gradient of adsorbed drug is generated from the outer layers of the aerogel (more concentrated) to the inner regions (less concentrated). This is particularly evident when low drug concentrations are used, the soaking time in the drug solution is short, and the exchange of the solvent by $scCO_2$ occurs slowly and some drug molecules can even move from inside to the surface [41]. Even if showing some drawbacks, this technique allows for reproducible drug

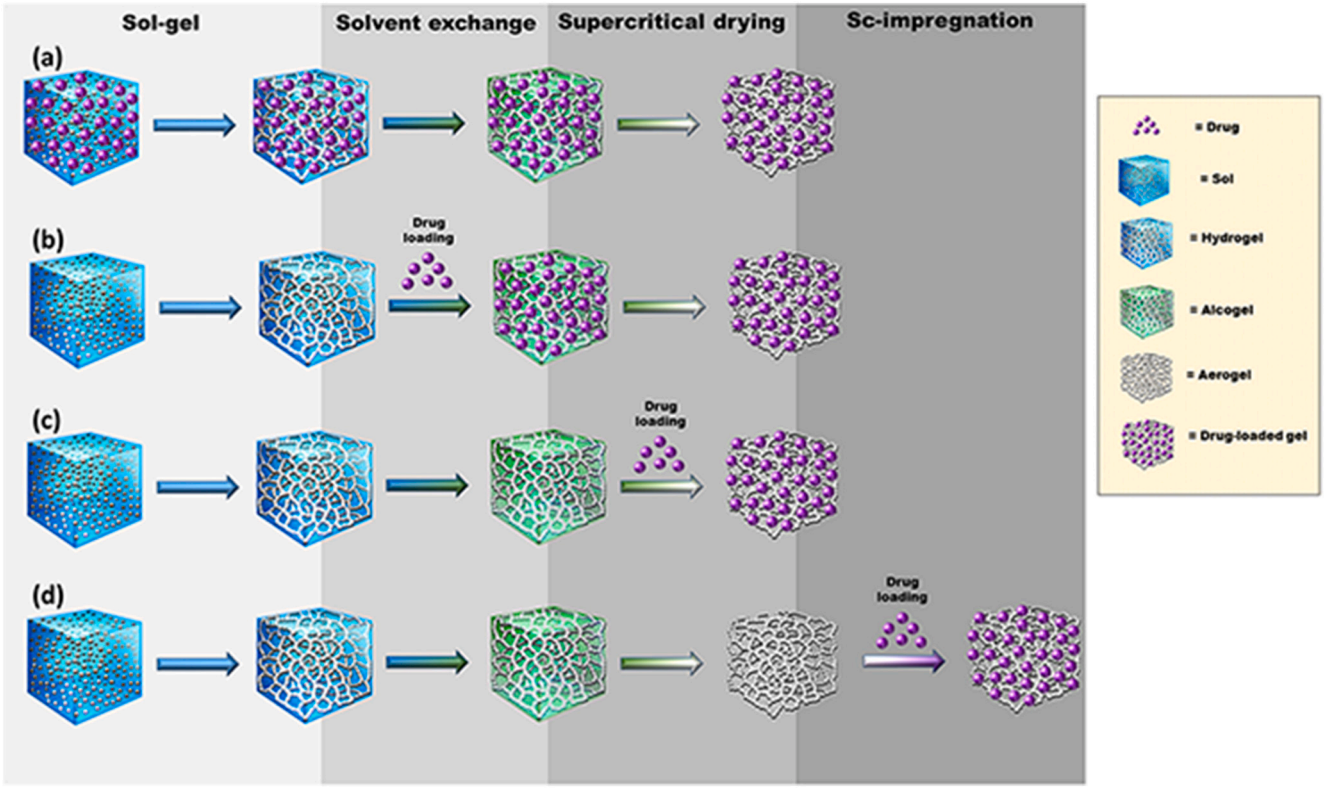


Fig. 2. Strategies to load drugs into aerogels: (a) the drug is added to the precursors solution; (b) the drug is added to the gel; (c) the drug is incorporated during the supercritical drying; and (d) the aerogel is formed first and then the drug is loaded.

crystallization in aerogels both in terms of drug loading and obtained polymorph.

(c) Drugs sensitive to common solvents but soluble in $scCO_2$ (e.g., acetylsalicylic acid or essential oils) can be loaded during aerogel formation in the supercritical drying step [42,43]. Improved knowledge on drug adsorption isotherms under supercritical conditions allows predicting the kinetics of the loading and the saturation values, as explained below [44,45].

(d) Formulation of drugs into preformed aerogels involves the exposure of the aerogel to liquid or gas phases containing the drug, which must diffuse through the pore network [34,46]. Immersion in aqueous or organic solvents may trigger aerogel deswelling or partial dissolution depending on the skeleton composition and also requires an additional step of solvent removal, with the risk of pore collapse and remaining of solvent traces that may lead to drug instability or toxicity. These drawbacks of extra processing steps together with the risk of losing the unique properties of the aerogel support the use of $scCO_2$ for the drug loading of preformed aerogels in case of drugs that dissolve in this solvent. Compared to other supercritical fluids, CO_2 is regarded as safe by the regulatory agencies for the processing of pharmaceutical and food products [47]. As advantageous features, CO_2 itself has low toxicity and low density, is noncombustible and can be recycled, and the supercritical conditions are achieved at mild values of pressure (7.4 MPa) and temperature (31.1 °C), which makes the process more economically convenient than other supercritical fluids [48]. Particularly, the processing temperature under $scCO_2$ medium can be close to that of human body, which may prevent the thermal degradation of temperature-sensitive therapeutic substances. For comparison, the critical point of water is 373.9 °C and 22.1 MPa [49]. Indeed, a large variety of hydrophilic and lipophilic drugs have been shown to withstand the processing under $scCO_2$ conditions [50]. $scCO_2$ is a non-polar solvent with low dielectric constant and, therefore, it cannot solubilize polar drugs and therapeutic proteins. Nevertheless, since $scCO_2$ can establish a variety of interactions with solutes, such as acid/base, dispersion, induced dipole, and quadrupole interactions, it becomes a suitable solvent for mid-polarity substances if the required concentration is relatively low [51,52]. Drug solubility can be enhanced either by increasing the pressure or by adding cosolvents (acetone, methanol, or ethanol). After processing, CO_2 evaporates fast, and no solvent traces remain in the aerogel. Preparation of water-in-CO_2 and oil-in-CO_2 emulsions has also been investigated to enhance the drug concentration using adequate surfactants and lipids [48]. Moreover, aerogel formation ($scCO_2$ drying) and subsequent drug impregnation can be integrated into a one-pot process [42].

The process of aerogel impregnation with drugs using supercritical fluids is known as adsorption precipitation [53]. A common protocol may be described as follows: (i) the aerogel monolith or particles (wrapped in a porous mesh) and the drug particles (directly or inside a permeable container) are placed together in a temperature-controlled pressurizable chamber; (ii) CO_2, solely or doped with cosolvents, is introduced in the chamber and the supercritical conditions are achieved; (iii) the drug is dissolved in the supercritical fluid and the penetration of $scCO_2$ into the aerogel pores facilitates drug diffusion; (iv) the drug is adsorbed on the interior surface of the aerogel (skeleton) and an adsorption equilibrium is reached if sufficient time is given (if desired), and (iv) after a given time of exposition under static or agitated conditions, the chamber is depressurized to remove CO_2 and any other solvent. Depending on whether the depressurization is slow or fast, the amount of drug adsorbed (deposited) on the aerogel may change. Slow depressurization (i.e., slow expansion) causes the precipitation of the drug that accessed the inner pores and was adsorbed onto their walls. The remaining drug that did not undergo adsorption may be dragged with the CO_2 or deposited on the chamber walls. Conversely, fast depressurization (i.e., rapid expansion) may cause a sudden decrease in the drug solubility as the solvent evaporates, which may promote enhanced deposition of drug particles onto the external layers of the aerogel. Depending on whether the drug molecules have sufficiently high affinity for the aerogel skeleton or the drug concentration in the medium is still very high, drug adsorption or precipitation predominates, respectively [53]. Readers interested in the advantages of using $scCO_2$ for the preparation of drug nanoparticles and nanocrystals are referred to a specialized review [51].

The knowledge of the mechanisms involved in the adsorption precipitation is crucial for tuning the rate, the amount and the crystalline state of the drug deposited into the aerogels. Non-swellable aerogels have extensively been studied in this regard [53]. In the sequence of pressurization-adsorption equilibrium-depressurization, the time to adsorption equilibrium is the rate-limiting step. Drug dissolution usually occurs in a few minutes, but diffusion through the supercritical fluid and into the aerogel and adsorption onto the skeleton may require between 10 and 24 h to reach equilibrium [54]. Diffusion coefficients for drugs that fulfil the rule of five set by Lipinski for molecules showing good oral adsorption [55] are in the 10^{-9}–10^{-8} m^2/s range [56]. The diffusion coefficient increases as the molecular weight of the drug decreases or a combined increase in temperature and decrease in pressure occurs. Regarding the amount of drug that can be adsorbed, common values range between 0.1 and 0.8 g/g [53], although remarkably larger amounts have been reported for eugenol (up to 8 g/g) in rice husk ash silica aerogel [57]. Drug solubility in the supercritical fluid is not the main factor regulating drug adsorption and indeed the amount loaded cannot be predicted from its solubility. Differently, the strength of the drug-skeleton interactions and even the drug-drug interactions may determine both the adsorption at equilibrium and the physical state of the deposited drug particles. As a rule of thumb, an increase in drug-skeleton affinity and a decrease in drug intermolecular interactions favor the deposition of amorphous drug in the pore walls. Also, the aerogel density has been suggested to play a key role in drug adsorption, although some contradictory results have been reported [58,59].

The information available also calls the attention on the challenges to characterize the nanocrystals confined within pores smaller than 1 μm, since they can become imperceptible using powder X-ray diffraction (XRD) techniques. Advantageously, the predominance of mesopores (2–50 nm) in the aerogel structure contributes to hinder the growth of the drug particles and minimizes the risk of drug crystallization, contributing to the stability of the amorphous particles or preventing crystal growth or polymorphic changes of drug nanocrystals.

Overall, the strengthening of the drug-skeleton interactions has also two direct positive consequences: (i) higher drug amounts can be loaded, and (ii) the likelihood that the drug remains in the amorphous state increases. In addition, the affinity of the drug for the aerogel skeleton can be enhanced through its functionalization with oppositely charged groups; namely acidic functionalities to load basic drugs, or amino and hydroxyl moieties to load acidic drugs. As an example, functionalization of silica aerogels with amine groups (gas phase functionalization) did not alter the density and porosity of the aerogel (surface area ~1000 m^2/g; 0.14 g/cm^3), but notably improved the adsorptive interactions with ketoprofen [60]. An increase in the content in amine groups from 1.06 to 2.98 wt% increased ketoprofen loading from 9.7 to 21.1 wt% due to specific interactions with the carboxylic acid group of the drug. The drug adsorbed did not show crystalline peaks and the release from the aerogels was faster than the dissolution rate of non-processed crystalline drug owing to its amorphization. Interestingly, a retarding effect of the amine group-drug interactions on drug release rate was not observed; on the contrary, the most functionalized aerogels led to even faster release rate. More recently, the molecular imprinting strategy has been also explored to increase the loading of drugs into aerogels through ad-hoc arrangement of the binding sites

[61].

2.2. Drug release mechanisms

Understanding drug release mechanisms is important to modulate the characteristics of the carriers and facilitate the design of new devices with advanced functionalities. General considerations can be formulated when the drug is physically deposited in mesoporous aerogels, but stimuli responsive systems where the active ingredient is chemically conjugated to the backbone have to be evaluated individually. This section deals only with the former systems. When the drug is dispersed on the surface and inside the pores of aerogel particles, drug release can be divided into two main mechanistic steps. The first step is the dissolution of the drug, which is followed by its transport from the device to the dissolution medium. Both processes are governed by several physicochemical factors that determine the limiting step in the mechanism, and eventually the rate of drug release. The most relevant factors are the following [62]: i) Hydration characteristics of the deposited drug and the carrier matrix, including erosion and swelling; ii) Specific interactions between the aerogel backbone and drug molecules; and iii) Mass transport processes effective in the hydrated delivery device. These factors have profound effects on both drug dissolution and transport, which should carefully be assessed in order to get a comprehensive understanding on drug release mechanism [63,64].

2.2.1. Hydration features

When the drug delivery device gets in contact with body fluids, the aerogel particles are hydrated starting on the surface and gradually penetrating into the pore network. Consequently, the deposited solid drug is also hydrated, which leads to its dissolution; first on the outer surface of the aerogel and afterwards inside the pores. The hydrophilicity of the drug and that of the aerogel carrier can be significantly different, taking into account that the characteristics of the drug significantly depend on its crystallinity as well. When a hydrophilic drug is loaded into a hydrophilic aerogel, hydration and drug dissolution are often fast, and the rate determining step in drug release is the mass transport of the dissolved drug from the outer surface and pores towards the release medium. On the other hand, the dissolution of hydrophobic active ingredients is usually slow even in their amorphous forms.

Aerogels are considered as highly hydrophilic if the backbone spontaneously absorbs water and develops a thick hydration layer, disregarding the solubility of the aerogel in water. Thus, in the case of highly hydrophilic aerogel carriers (e.g., polysaccharides, proteins, silica, and alumina), the facile hydration of the backbone effectively drives the displacement of the deposited drug, which considerably increases dissolution rate. In the same line of thoughts, when the aerogel carrier is hydrophobic (e.g. hydrophobized silica or biopolymers), its hydration is hindered, which usually results in the retarded release of active ingredients.

Besides facilitating drug desorption, the facile hydration of hydrophilic aerogels can lead to erosion, swelling, and in some cases, dissolution of the carrier matrix. Inorganic oxide (e.g., silica, alumina, titania) and crosslinked (bio)polymer aerogels are usually very hydrophilic, but they do not swell upon hydration and their open mesoporous structure remains intact in water [65]. Mass transport into and out of these hydrated aerogel particles is practically unhindered due to the conserved highly interconnected open porous system. Another effect to be considered is that inorganic oxide aerogels tend to erode spontaneously in water yielding microparticles of 10–40 μm. Matrix erosion of the wet aerogel can be complete in 1–30 min in a stirred vessel. The fast erosion of bulk aerogels to microparticles with open pores usually results in the rapid release of loaded drugs. This is effective in most of the inorganic oxide based aerogel carriers. The erosion of hydrophobized aerogels in an aqueous milieu is slower.

Differently, biopolymer aerogels undergo extensive structural changes upon wetting and hydration. When completely hydrated, carbohydrate and protein aerogels tend to swell due to the rearrangement of the backbone, which finally results in the collapse of the pores and the formation of a hydrogel-like matrix. Because the collapse of the pore system is often fast, the swollen particles can entrap much of the loaded drug. In these cases, hindered diffusion from the hydrogel-like particles controls the rate of drug release. In extreme cases, the rate limiting process is the dissolution of the hydrated carrier matrix. These effects usually result in retarded drug release from biopolymer aerogels that swell in aqueous media. In sum, if hydrogel formation is fast, the loaded drug will be trapped in the hydrogel. If hydrogel formation is slow, the drug may dissolve and leave the porous structure before the collapse of the pores (and the formation of a hydrogel layer).

It is important to emphasize that the dissolution of drugs and the hydration of aerogels, including erosion and/or swelling, depend on the chemical properties of the release medium. The most important properties are pH, temperature, ionic strength and the presence of surfactants. A high variation in swelling or solubility can be utilized for developing stimuli responsive carriers. For example, chitosan and poly (N-isopropyl acrylamide) (PNIPAM) show, respectively, significant pH- and temperature-dependent swelling and aggregation [66,67]. In general, drug release is faster under such conditions where the pores of the carrier matrix remain open, and release is retarded when the pores collapse due to swelling. In addition, drug release is faster when the conditions favor the dissolution of the carrier. Details on stimuli responsive aerogel carriers are given later in Section 3.2.

The different hydration characteristics of inorganic and biopolymer aerogels can be combined and utilized to tune drug release rate. One strategy is coating the porous carrier with biopolymer layers that swell. In these systems, hindered mass transport through the outermost hydrated biopolymer layer, and in the later stages, the dissolution of the layer determine the rate of drug release. It has been shown that the release of deposited curcumin is fast from pectin aerogel carrier. However, prolonged drug release was achieved by coating the loaded pectin aerogel with chitosan. A compact hydrogel layer forms from chitosan in water, which limits the transport of the dissolved drug into the release medium [68]. The feasibility of encapsulating silica aerogel with a tunable alginate aerogel layer has been explored too [22]. Additional examples for coated and core-shell aerogels are given later in Section 3.3.

Another strategy for controlled release is fusing the different hydration properties of inorganic and organic materials by hybridization. A variety of silica-casein and silica-gelatin aerogels has recently been prepared utilizing co-gelation as part of the sol-gel method in synthesizing the gel network of the aerogels. These hybrids are homogeneous on the nanoscale. Interestingly, silica-casein aerogels do not swell, and retain their open porous structures in water [69]. Silica-gelatin hybrid aerogels of low (<5 wt%) gelatin content do not significantly swell upon hydration, but the facile hydration of the backbone drives the rapid displacement of loaded hydrophobic drugs (e.g. ibuprofen and ketoprofen). Therefore, rapid release is characteristic for low gelatin content hybrids [70]. On the other hand, silica-gelatin aerogels of high (>20 wt %) gelatin content significantly swell in water, which results in the entrapment of loaded drugs and retarded drug release. Owing to these effects, drug release rate can be tuned by changing the ratio of the inorganic and organic components of the hybrid aerogel carrier, as seen in Fig. 3 [71]. The most studied strategies for controlling the hydration of aerogels is hydrophobization and crosslinking. In general, hydrophobization slows down the wetting of the aerogel matrix, and its limited hydration prevents erosion. Controlled hydrophobization has been explored in tuning the release properties of silica, inorganic-organic hybrid and biopolymer aerogels [72–74].

2.2.2. Specific interactions

Every interaction between the aerogel backbone and the drug molecule is considered specific besides dispersion forces and dipole-dipole interactions. The most common interactions are hydrogen

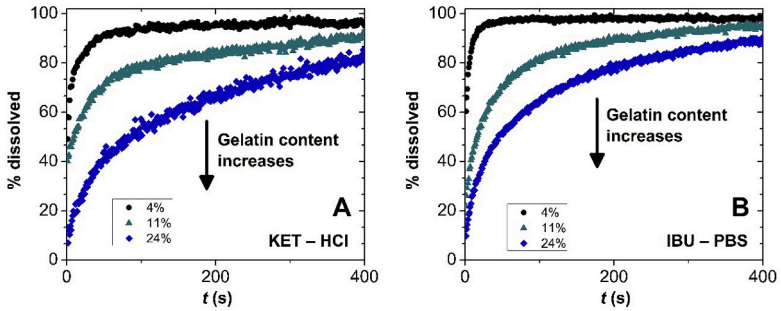


Fig. 3. Release of deposited (A) ketoprofen in HCl (pH 1), and (B) ibuprofen in phosphate buffer saline (PBS, pH 7.2) from silica-gelatin aerogels of varying gelatin content, as shown in the legend. Drug release is diffusion limited from aerogels of high gelatin content due to the swelling of the carrier matrix and the encapsulation of the drug. Low gelatin content aerogels do not swell, and drug release is significantly faster. Reprinted from Keri et al. [71] with permission from Elsevier.

bonding and ionic bonding, but coordination bonds (e.g. with metal ion containing drugs) and supramolecular interactions are possible as well. The nature of specific interactions heavily depends on the chemical structure and physical states of the drug and the aerogel. The physical state, e.g. the crystallinity of the components, is determined by the conditions of aerogel synthesis and drug deposition. When the carrier device becomes hydrated, the chemical conditions in the release medium (pH, temperature, ionic strength, presence of surfactants) have profound effects on the nature of specific interactions, via the change of the conformation, protonation state, surface charge density (estimated by the zeta-potential) of the drug molecule and the aerogel backbone [69].

Strong interaction between the drug and the aerogel results in establishment of dynamic adsorption-desorption equilibrium between free and bound drug molecules. The rate of drug release is governed by the kinetic characteristics (lability) of the interfacial equilibrium, and the retained amount of drug is determined by the thermodynamic stability of the bound state. Drug adsorption is not favored on hydrophilic aerogels in aqueous media due to the facile hydration of the backbone, thus only a small portion of the drug is retained by the carrier matrix in equilibrium in most cases [75]. Ensuring sink conditions also effectively shifts the interfacial equilibrium towards desorption of the drug. It is important to note that a high kinetic barrier can exist for drug detachment, which can significantly decrease drug release rate. Desorption of H-bonded drug molecules is thermodynamically favored due to hydration of binding sites, but the process is nevertheless, slow. In such cases, desorption can become the rate controlling step in drug release [74]. It was shown in the case of polyurea crosslinked random porous dysprosia aerogels that two processes are operational in determining release rate of loaded active ingredients (paracetamol, indomethacin, and insulin). The first process is the diffusion of dissolved drug molecules out of the pores, and the second process is the desorption of the H-bonded molecules. Drug molecules close to the surface of the particles escape rapidly by diffusion. However, drug molecules deep in the small pores in close interaction with the aerogel skeleton are bound by H-bonds. The release rate is limited by the slow breaking of the H-bonds, resulting in equilibrium desorption. These effects are spectacularly reflected in the dual character of the cumulative release curves (Fig. 4) [76].

2.2.3. *Mass transport processes*

As discussed above, aerogels can erode, swell and collapse in contact with water. Importantly, effective mass transport in a drug delivery device is governed by the structure of the wet device, which can be very different from that of the dry aerogel. As an approximate trend, those

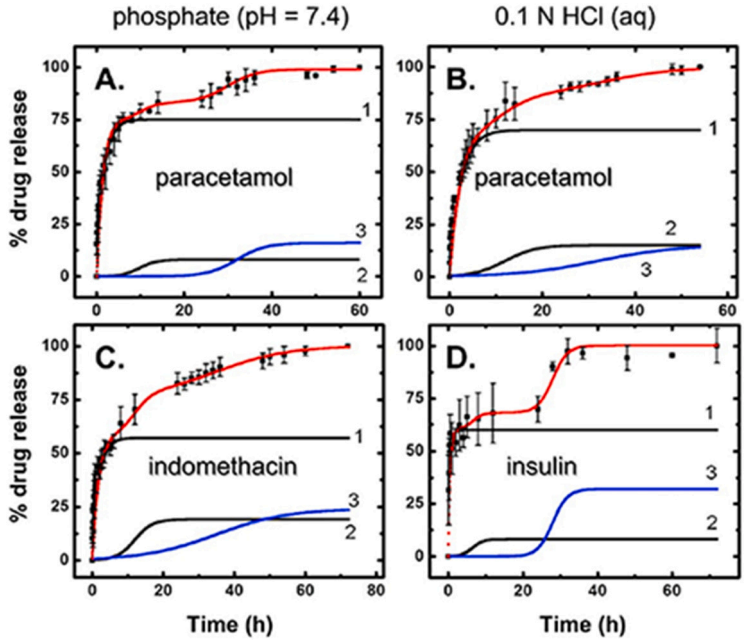


Fig. 4. Release of active ingredients from polyurea crosslinked random porous dysprosia aerogels. The dual character of the release curves reflects that a portion of the drug is retained in the carrier due to the formation of strong H-bonds with the aerogel skeleton. Reprinted with permission from Bang et al. [76]. Copyright (2014) American Chemical Society.

aerogels that extensively erode do not swell or collapse (e.g. silica, alumina, cross-linked biopolymers), and erosion is negligible in those aerogels that extensively swell or collapse in water (e.g. natural biopolymers).

In case of such aerogels that preserve their open porous structure in water, the rate limiting step in release is either the diffusion of water into the aerogel to dissolve the drug, or the diffusion of dissolved drug out of the particles. The diffusion of water into the pores is hindered in hydrophobic aerogels. Thus, the hydration of the device and the dissolution of the drug often limit the rate of drug release from hydrophobized silica and biopolymer aerogels. Unfortunately, modeling studies rarely deal with the rate of hydration of (hydrophobic) aerogel particles with respect to drug release mechanisms. In case of hydrophilic aerogels, the hydration of the carrier device and the dissolution of the deposited (amorphous or nanocrystalline) drug is usually much faster than the diffusion of drug molecules in the pores towards the release medium. In these cases, the factors regulating drug diffusion pathways (e.g., pore size and geometry, bottlenecks, tortuosity, length of channels) regulate the release rate. Therefore, the well-established semi-realistic models of drug release (e.g. Higuchi, Peppas, Korsmeyer, Hopfenberg) can usually be applied to hydrophilic open porous aerogel particles. These models are based on the mechanism of Fickian diffusion and take into account the distribution of the drug in the device and the shape of the device. In extreme cases, when the erosion of the aerogel is very fast, the rate of drug release can be proportional to the increasing net surface of the carrier device. The derivation, the general use and the limitations of such models are discussed in length in several review and opinion papers [63,64,77]. The application of simple semi-realistic models to describe drug release from aerogels is demonstrated through selected examples in the next section.

Biopolymer aerogels swell and collapse in water leading to the formation of hydrogel-like particles. Most often, the hydration of the aerogel and the dissolution of the drug are very fast. When the collapse of the pore structure is faster than the diffusion of dissolved drug, the drug molecules are entrapped in the hydrogel-like matrix. In these situations, drug release becomes diffusion limited and modeling is often successful based on the mechanism on Fickian diffusion. Cumulative drug release can usually be described in these systems with the corresponding semi-realistic models, such as the Korsmeyer-Peppas model [46].

Interestingly, the rate limiting process can change even within one family of aerogels by the variation of aerogel structure. Silica-gelatin hybrid aerogels of low gelatin content are eroding carrier devices, but the rate of drug release becomes diffusion limited with the increase of the gelatin content of the carrier because of more and more expressed swelling. The mechanism change is reflected in the change of the shape of the release curves, as seen in Fig. 3 [71].

2.2.4. Mathematical drug release models

Simple semi-realistic models can be utilized to describe cumulative drug release from aerogel carriers only in the most fundamental cases, because drug deposition into the aerogels without specific interaction with the skeleton and in the crystalline state is quite unlikely (see 2.1 (b) above). However, in this particular situation and for aerogels where erosion, swelling or collapse are either negligible or very well-defined, the drug release rate can be quite easily predicted and modeled, as discussed in the previous section. In these fundamental cases, mass transport processes can be combined into a single kinetic term, which leads to the well-known simple mathematical formulations, e.g., Higuchi, Peppas, Korsmeyer, Hopfenberg, and first-order models [63,64,77].

A good example is drug release from bacterial cellulose aerogels [78] that was perfectly predicted by Fickian diffusion equations, assuming that (i) the diffusion length is half of the thickness of the gel, and that (ii) once a certain water content is reached in a region of the matrix, the diffusion of the drug molecule starts [79]. Bacterial cellulose pre-gels were loaded with dexpanthenol and L-ascorbic acid (vitamin C) by soaking into the respective drug ethanolic solutions and subsequently dried using $scCO_2$ to obtain the aerogels with the drug precipitated inside [78]. Loading isotherms showed a linear dependence of the amount of drug deposited in the aerogel and the drug concentration in the soaking solution, which suggested the absence of specific drug-cellulose interactions. Release profiles were recorded in water. Differently to many other biopolymer aerogels, bacterial cellulose aerogels did not collapse when immersed in water, therefore maintained their open porous network, which facilitated the access of water to the full structure. Thus, the release could be explained in terms of diffusion of the dissolved drug molecules from the inner aerogel to the release medium and, indeed, the rate was shown to depend on the thickness of the aerogel monolith (Fig. 5).

The Korsmeyer model [79], which considers simultaneous water diffusion into an open-porous matrix and drug diffusion out of it, fitted quite well the release profiles. In the case of bacterial cellulose aerogels, since no changes in volume occur during the release, the contribution of swelling to the release pattern can be neglected [78]. Diffusion has also been shown to be the main mechanism of curcumin release from non-swellable aerogels made of a polyvinylidene fluoride-hexafluoropropylene (PVDF-HFP) copolymer, and the release rate was regulated via an increase in polymer concentration, which increased the tortuosity of the diffusional pathway [80]. Similarly, ibuprofen release from silk fibroin aerogels that did not swell or lose any weight in phosphate buffer saline (PBS) of pH 7.4 in the time frame of their capability to sustain drug release (6 h) was perfectly modeled by Fickian diffusion [81].

The procedure followed to load the drug into the aerogels has also been shown to impact not only the drug adsorption yield, but also the drug release pattern because it changes the interactions between the cargo and the matrix. In a comparative study carried out with silica and alginate aerogels, *Clinacanthus nutans* (*C. nutans*) plant extracts were loaded either by wet impregnation (extracts obtained using ethanol or ethanol/water mixture) or supercritical impregnation with the main extract component phytol [82]. Silica aerogels exhibited the highest loading after supercritical impregnation, while alginate aerogels showed remarkably better loading when impregnated with the extracts. Alginate aerogels had the highest loading amounts under all conditions, disregarding their smaller surface area compared to silica aerogels (126 vs. 881 m^2/g), which again revealed that not only the physical properties but also the nature of the aerogels may determine the adsorption of the active substances [52]. Importantly, phytol release tests (PBS pH 6.8, 37 °C) with $scCO_2$-impregnated aerogels evidenced the irreversible binding of the active compound to the aerogel skeleton [82]. Alginate aerogels impregnated with ethanol extracts (loading of 18.5 wt%) showed sustained release profiles, while those impregnated with ethanol/water extracts (loading of 9.6 wt%) released the components much faster, although still with a controlled pattern (Fig. 6). The efficient loading of phenols and flavonoids from the extract suggested that the interactions between alginate and the hydrophobic compounds of the extract are quite strong. These interactions together with the low solubility in water of the components extracted in ethanol explain the slower release recorded for the alginate aerogels impregnated with the ethanol (100%) extract. Release patterns of both formulations fitted quite well to the Higuchi model (diffusion-controlled release) but, since swelling and erosion of aerogels were observed, the profiles were also fitted to the power-law model [83] (Eq. (1)),

$$\frac{M_t}{M_\infty} = kt^n \quad (1)$$

In this equation, M_t represents the amount released at time t with respect to the total amount loaded (M_∞), k is the release rate coefficient and n is an index of the release mechanism. The fitting revealed values of n of 0.61 for the formulation impregnated with the ethanol (100%) extract, indicative of anomalous (non-Fickian) diffusion.

Very fast drug release takes place when there is practically no specific interaction between the drug and the aerogel, and the aerogel does

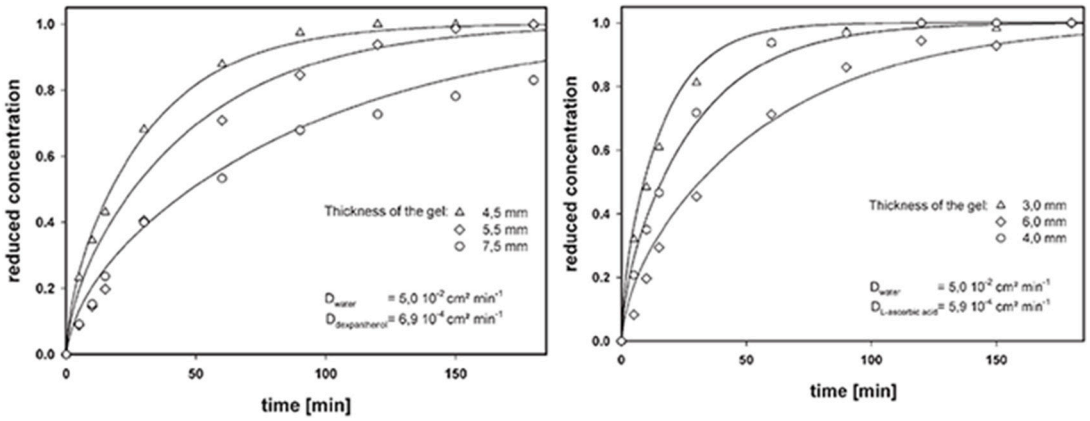


Fig. 5. Release profiles in water of dexpanthenol (left) and L-ascorbic acid (right) from bacterial cellulose aerogels of different thickness that had been loaded with the drug by immersion of the alcogels in a drug solution and then underwent $scCO_2$ drying. Reprinted from Haimer et al. [78] with permission from John Wiley and Sons.

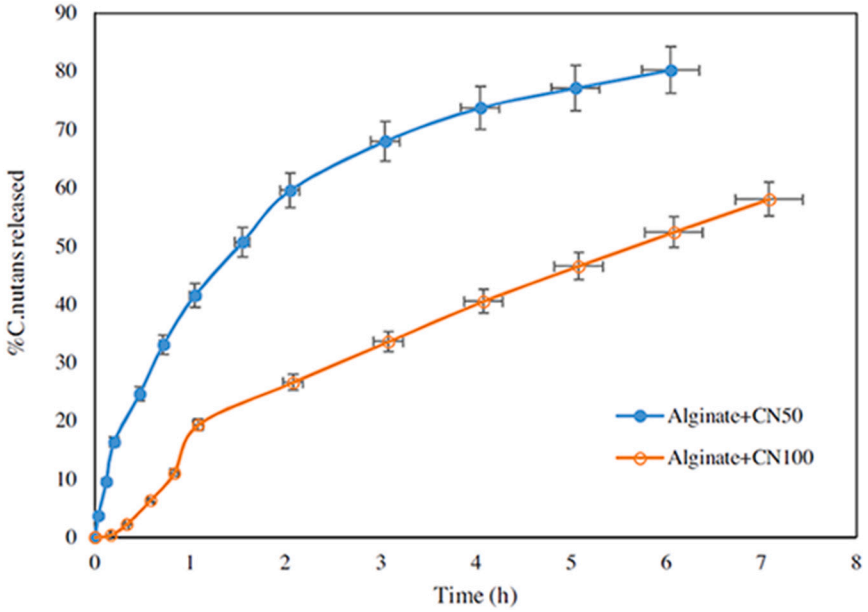


Fig. 6. Release pattern of *Clinacanthus nutans* (*C. nutans*) plant extract from alginate aerogels loaded by wet impregnation with extracts in 100% ethanol (CN100) or 50% ethanol (CN50). Reprinted from Mustapa et al. [82] with permission from Elsevier.

not swell or collapse, but rapidly erodes due to hydration. These conditions are realized when hydrophobic drugs are deposited into hydrophilic inorganic (e.g. silica) aerogels. The hydration and the consequent erosion of the aerogel are very fast and lead to the formation of open porous microparticles. Consequently, drug dissolution and diffusion out of the small particles are fast due to the large specific interface with the release medium. In such extreme cases, drug release rate is proportional to the time-dependent net surface area of the eroding device. Cumulative release can be modeled by a semi-empirical equation proposed by Hopfenberg [84] (Eq. (2)),

$$\frac{M_t}{M_\infty} = 1 - \left(1 - \frac{k_0 t}{c_0 r}\right)^n \quad (2)$$

In this equation, c_0 is the initial loading of the drug dispersed uniformly in the device, r is the characteristic dimension of the device (e.g., the radius of spherical particles), n is a shape factor representing spherical ($n = 3$), cylindrical ($n = 2$) or slab geometry ($n = 1$), and k_0 is a zero-order rate constant. The Hopfenberg model was originally derived for surface eroding carriers, where all mass transport leading to drug release add up to a zero-order process focused on the surface of the device. This model successfully describes the rapid release of ibuprofen and ketoprofen form quasi-spherical silica based aerogel particles, where facile hydration drives the detachment of the drug and the erosion of the device [71] (Fig. 7).

In a case study, a series of mesoporous silica aerogels with varying density were synthesized and loaded with ketoprofen in $scCO_2$ [85]. The mean pore size showed an inverse correlation with aerogel density, but loading was approximately the same for all aerogels (between 16 and 23 wt%). Drug release in 0.1 M HCl medium was approximately five times faster than the dissolution of the pure drug, and it was the fastest from silica aerogel of the lowest density (0.033 g cm^{-3}) and largest mean pore size (24 nm). Cumulative release was successfully modeled by the first-order equation (Eq. (3)),

$$\frac{M_t}{M_\infty} = 1 - exp(-k_1 t) \quad (3)$$

In this equation k_1 is the first-order rate coefficient describing the combined effect of mass transport processes controlling release rate.

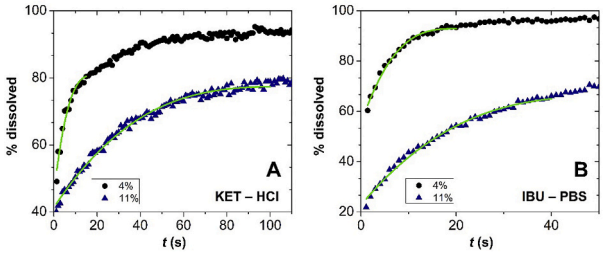


Fig. 7. Rapid release of deposited ketoprofen (KET) in HCl pH 1.0 (A) and ibuprofen (IBU) in PBS pH 7.2 (B) from silica-gelatin aerogels of low gelatin content (given in the legend). Drug release rate was proportional to matrix erosion rate, and cumulative drug release was successfully simulated using the Hopfenberg model (Eq. (2)). Continuous lines show the best fits. Reprinted from Keri et al. [71] with permission from Elsevier.

As discussed in Section 2.2.2, random porous and hierarchically porous polyurea crosslinked silica aerogels and dysprosia aerogels were loaded with paracetamol, indomethacin or insulin. The release of these active ingredients was investigated in 0.1 M HCl and in PBS media, yielding complicated multi-step release curves (Fig. 4). Nevertheless, release curves were successfully fitted with the first-order model complemented by two additional sigmoidal components as additive terms. The mechanistic explanation is that the release of drug molecules closer to the surface is governed by diffusion (first-order term), but drug molecules deep in small pores are in adsorption-desorption equilibrium (sigmoidal terms) due to strong H-bonding with the aerogel skeleton [76].

As a final point, it has to be mentioned here that the effects of hydration, specific interactions and mass transport have already been combined successfully into single comprehensive realistic models that give unprecedentedly deep mechanistic insights into drug release from porous silica carriers [86,87]. However, the application of these models is limited to very specific systems, and has to be re-evaluated for each carrier and drug combination in order to gain the desired mechanistic insights.

3. Aerogels for oral administration

Oral drug bioavailability depends on a very delicate balance among dose, solubility, permeability and pre-systemic metabolism [55,88]. Therapeutic outcomes may be notably enhanced when the drug is targeted to or released in a specific region of the gastrointestinal tract that is more favorable in terms of drug physicochemical stability and/or permeability [89]. Additionally, the maintenance of drug levels for a prolonged time is required for drugs with narrow therapeutic index and for chronic treatments, which demands the development of oral formulations able to precisely regulate the release rate [90]. In addition, reducing the administration frequency could be achieved by prolonging the residence time of the delivery system in the gastrointestinal tract by means of mucoadhesion, for which mucoadhesive polymers and particulate formulations could be used [91]. Examples of aerogels that can successfully contribute to the achievement of the above reported desired performances are analyzed in the next subsections.

3.1. Aerogels as drug solubilizing aids

Drugs that exhibit solubility values that prevent complete dissolution of the required dose in a reasonable time frame for oral absorption are classified as Class II or Class IV in the Biopharmaceutics Classification System (BCS) depending on whether the membrane permeability is high or low, respectively [88]. More than 40% of current drugs on the market are poorly-water soluble, which limits the amount that can be orally absorbed and, in turn, the bioavailability and the therapeutic efficacy. Low aqueous solubility also challenges the formulation and preclinical and clinical evaluation of most of the new chemical entities [92].

Among the wide variety of drug solubilization strategies, preparation of solid dispersions or complexes (e.g., cyclodextrins, polyelectrolytes) in which the drug molecules remain individualized or as amorphous small particles has largely been proved successful to enhance drug dissolution rate and apparent solubility in the gastrointestinal fluids after oral administration [93]. Similarly, drug loading into aerogels using supercritical fluids commonly leads to aerogels impregnated with amorphous drug particles. Drug formulation in silica or hydrophilic biopolymer-based aerogels has also been shown to increase dissolution rate mainly due to drug amorphization and a sharp increase of the surface area. However, in the case of aerogels, the term solid dispersion is not accurate since drug molecules or particles remain adsorbed onto the pore walls. They are not integrated into the aerogel skeleton itself but dispersed onto its surface [53].

Differently to the drug recrystallization commonly observed when the aerogels are processed by freeze-drying [40], the interactions of the drug molecules with the aerogel skeleton and the confinement of solid drug particles (either as amorphous or as nanocrystalline metastable polymorphs) notably prevent crystal growth and recrystallization into stable polymorphs [94]. Table 1 summarizes relevant examples of the interest of aerogels as fast or immediate release oral dosage form.

Early reports on $scCO_2$ impregnation of hydrophilic silica aerogels with drugs evidenced the capability of the mesopores to host a variety of molecules of different polarity: ketoprofen, miconazole, terfenadine, dithranol, niclosamide, griseofulvin, and nimesulide, among others [54,72]. After impregnation, the drugs remained in amorphous state, which notably enhanced the dissolution rate (4-5-fold) either in 0.1 N HCl or PBS pH 7.4, compared to the unprocessed crystalline drug particles. Hollow silica aerogel microspheres prepared from rice husk ash (338.9 m^2/g surface area and 1.7 cm^3/g pore volume) and impregnated with ibuprofen (0.47 g/g) using $scCO_2$ released 80% of the drug payload within the first 15 min after immersion in 0.1 N HCl solution doped with 1% sodium dodecyl sulfate (Table 1, entry 1). The unprocessed crystalline drug dissolved only 11% in the same time interval [95]. Subsequent improvements in the structure of the microspheres allowed for 100% ibuprofen release in 15 min [96]. Hydrophilic aerogel microspheres from rice husk ash generated with optimized composition and sol-gel emulsion conditions showed improved capability to adsorb ibuprofen (up to 0.87 g/g) both as amorphously dispersed and as nanocrystals [57]. The aerogels had a burst release of ~80% of the loaded drug in the first 30 min followed by a sustained release. The coexistence of fast dissolving amorphous drug and small crystals with high surface contact area with the release medium together with a fast disintegration of the microspheres explain the fast release.

Since silica aerogels are biocompatible but the biodegradability and fate in human body are highly variable [97], hybrid systems with biopolymers and biopolymer-solely aerogels are gaining increasing attention for drug formulation. In a comprehensive research, fourteen hybrid aerogels prepared with different silica/gelatin ratios were investigated as drug solubility enhancers [74]. The aerogels were prepared by combining silica and gelatin and, then, hydrophobic moieties were introduced to tune the stability in contact with aqueous medium and also the strength of the interactions with three low solubility, weakly acidic drugs chosen for the study: the nonsteroidal anti-inflammatory (NSAID) drugs ibuprofen (pK_a = 4.40) and ketoprofen (pK_a = 4.76), and the antiplatelet agent triflusal (pK_a = 4.15) (Table 1, entry 2). An increase in the gelatin content from 3% to 24% caused a decrease in surface area from 700 to 300 m^2/g and in pore volume from 2.1 to 1.2 cm^3/g. Triflusal, the drug showing the highest solubility in $scCO_2$, was adsorbed to a larger extent (0.25–0.29 g/g) compared to ibuprofen (0.19–0.24 g/g) and ketoprofen (0.11–0.15 g/g). The increase in hydrophobic groups did not enhance drug loading but caused a slight decrease. XRD and differential scanning calorimetry (DSC) analysis suggested that the drugs were molecularly dispersed on the inner surface of the aerogel. Drug solubility tests were carried out in media of pH 2.0

Table 1
Examples of aerogels suitable for fast or immediate oral release reported in the last decade.

Entry	Aerogel composition	Drug	Loading method	Release conditions and outcomes	Reference
1	Hollow rice husk ash silica aerogel microspheres	Ibuprofen	$scCO_2$ impregnation of preformed aerogel	0.1 N HCl with 1% sodium dodecyl sulfate. Faster drug release than crystalline drug (80% vs. 11% in 15 min)	[95]
2	Silica and gelatin hybrid aerogels with various functionalities	Ibuprofen, ketoprofen and triflusal	$scCO_2$ impregnation of preformed aerogel	pH 2 and 6.7 medium. Aerogels showed burst followed by sustained release at acid pH and rapid release at pH 6.7	[74]
3	Alginate	Ibuprofen	$scCO_2$ impregnation of preformed aerogel	Buffer pH 7.2. Compared to crystalline ibuprofen, alginate aerogels showed faster release rate (<90% in 2 h)	[35]
4	Carrageenan cross-linked with KCl	Ibuprofen	$scCO_2$ impregnation of preformed aerogel	Buffer pH 7.2. Compared to crystalline ibuprofen, the aerogels showed immediate release	[99]
5	Alginate	Ketoprofen	Dug added to alginate dispersion before cross-linking	0.1 M HCl for 2 h, then phosphate buffer pH 6.8. Burst at acid pH and complete release in few minutes at pH 6.8	[100]
6	Alginate	Ketoprofen, nimesulide, and loratadine	$scCO_2$ impregnation of preformed aerogel	Release tests in pH 6.8. Ketoprofen and nimesulide dissolved in less than 30 min at pH 6.8. Loratadine dissolved in 5 min at pH 1.2.	[101]
7	Maize starch	Ketoprofen, nimesulide, and diclofenac	$scCO_2$ impregnation of preformed aerogel	Phosphate buffer saline pH 7.4. Complete release in few hours.	[102]
8	Silica, starch, alginate	Ibuprofen	$scCO_2$ impregnation of preformed aerogel	Phosphate buffer pH 6.8. More than 90% released in 30 min.	[103]
9	Maize starch	Vitamin E and vitamin K3	$scCO_2$ impregnation of preformed aerogel	Phosphate buffer pH 7.4. The aerogels shortened to approx. 1 h the dissolution time.	[106]

(10 mM HCl) and pH 6.7 (PBS). As expected, unprocessed crystalline ibuprofen, ketoprofen and triflusal particles exhibited a remarkable pH-dependent solubility; the solubility at pH 2 being 0.06, 0.26 and 0.69 mg/mL, respectively. At pH 6.7, the particles readily dissolved, and the solubility was above 0.70 mg/mL. Triflusal is highly unstable in neutral-alkaline aqueous medium, but encapsulation within silica aerogels was previously demonstrated to enhance drug stability during storage for 6 months at 21 °C and 60–65% relative humidity (RH) due to the acidic environment provided by the SiO_2 matrix [98]. Encapsulation within hybrid silica/gelatin aerogels without hydrophobic moieties led to a burst of more than 50% released at pH 2 in the first hour, and to a nearly complete release at pH 6.7 in the same time frame. Hydrophobically modified (silylated) aerogels showed more sustained release, particularly at pH 2 (Fig. 8), due to a strengthening of the drug-matrix interactions through hydrogen bonds.

Improvements in ibuprofen release rate have also been observed after $scCO_2$-impregnation of alginate aerogels (Table 1, entry 3) [35] and carrageenan aerogel microparticles (65–154 μm) obtained via the emulsion-gelation technique (Table 1, entry 4) [99]. Carrageenan aerogel microparticles contained the drug in amorphous state and provided

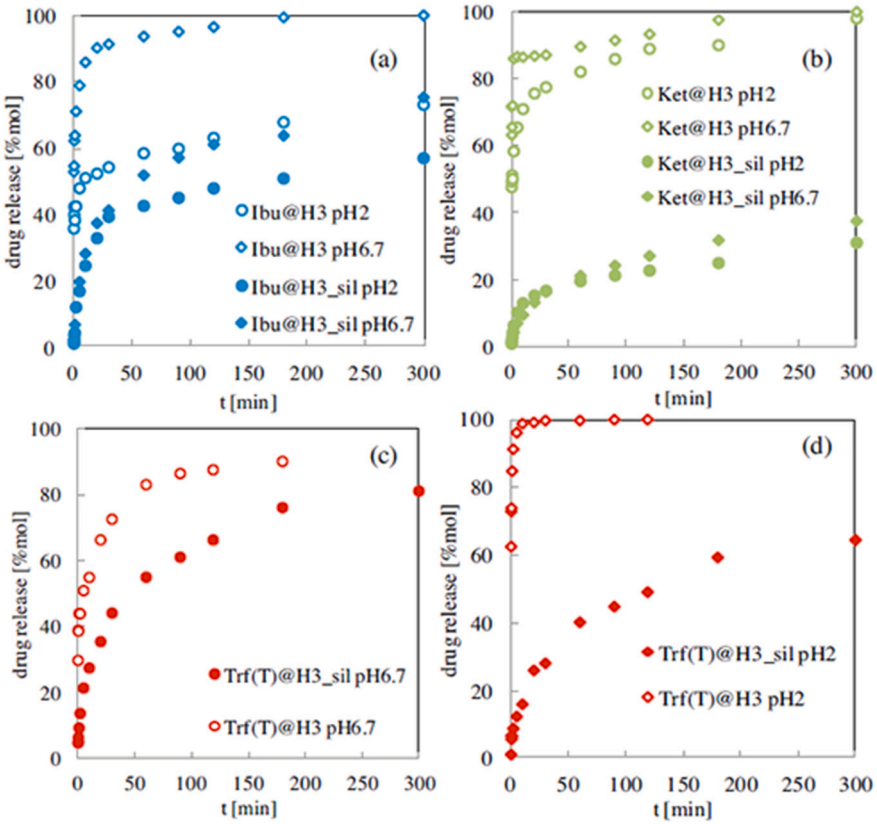


Fig. 8. Release profiles of ibuprofen (Ibu), ketoprofen (Ket) and triflusal (Trf) from hybrid silica/gelatin (3 wt%) aerogels without hydrophobic groups (H3) or with silylated groups (H3_sil) recorded at 37 °C and pH 2 or pH 6.7. Reprinter from Veres et al., [74] with permission from Elsevier.

>90% release in less than 10 min (PBS pH 7.2). Interestingly, the authors carried out physical and chemical stability studies by placing the ibuprofen-loaded aerogels in amber glass bottles in chambers at 30 and 40 °C and 75% RH for 3 months. The aerogels remained chemically stable but, depending on the carrageenan type and the relative amount of drug loaded, crystallization of ibuprofen was observed at 40 °C. It was suggested that aerogels prepared with kappa-carrageenan and low drug contents had adequate physical stability and prevented better drug crystallization than the other counterparts [99]. Nevertheless, drug release profiles after storage were not re-evaluated.

As an alternative to emulsion preparation, spherical aerogel particles can be generated by prilling, i.e. using a vibrating nozzle device that produces fine droplets, which avoids oil phase removal and could be more easily scaled-up. Precisely sized drops of alginate solution containing ketoprofen were collected in a bath containing the cross-linker in an aqueous medium or in ethanol, and dried using $scCO_2$ after solvent exchange. The obtained aerogels (2.5–3.1 mm) showed excellent sphericity [100]. Aerogels cross-linked in the aqueous medium contained ketoprofen in amorphous state and showed fast release (75% dose in 30 min) when immersed in simulated gastric fluid (Table 1, entry 5). Xerogels of similar composition but dried in a conventional oven (shrunk structure) only released 20% of the cargo after 120 min. Aerogels cross-linked in ethanol had ketoprofen in crystalline state and the release pattern was intermediate to the other formulations, with 40% dose released in 30 min. Using a similar approach, dripping of alginate solution into the crosslinking bath and subsequent $scCO_2$ drying and drug impregnation has been proved useful to produce aerogels particles (2.7 mm; 512 m^2/g) loaded with ketoprofen (18–28 wt%), nimesulide (5–14 wt%) or loratadine (24–30%) [101]. The drugs remained in amorphous state for six months of storage. Release tests in pH 6.8 medium evidenced that ketoprofen and nimesulide can be fully dissolved in less than 30 min. Loratadine release in pH 1.2 medium was completed in less than 5 min (Table 1, entry 6). These fast release profiles were in good agreement with those reported for nimesulide, ketoprofen and diclofenac sodium when $scCO_2$ impregnated into monoliths of maize starch aerogel [102] (Table 1, entry 7).

The impact of the role of the aerogels as drug solubilizing aids was evidenced for ibuprofen as a remarkable increase in oral bioavailability. Compared to an oral suspension of the unprocessed free drug, the formulation of ibuprofen in silica, starch or alginate aerogels accelerated drug release rate (Table 1, entry 7) and increased more than 2-fold the relative bioavailability [103] (Fig. 9). Similarly, encapsulation of the antifungal itraconazole in starch aerogels provided a 3-fold increase in relative bioavailability compared to marketed products [104]. Oral bioavailability of phytosterol has been also shown to increase from 3% when the crude crystalline compound was directly administered, to 35% when supercritically impregnated into starch aerogels [105].

A maize starch-based aerogel has been shown suitable for loading high amounts of lipophilic vitamin E (α-tocopherol) and vitamin K3 (menadione) using $scCO_2$ adsorption [106]. Solubilities of vitamin E and vitamin K3 in $scCO_2$ at 15 MPa in the 40 to 60 °C interval were in the 3–8 and 1.5–2 mg/g range, respectively. The adsorption isotherms revealed the remarkable effect of temperature (40 °C/15 MPa or 60 °C/15 MPa) on the adsorption isotherms (Fig. 10). The aerogels showed a highly efficient loading (145 mg vitamin E/g and 100 mg vitamin K3/g), and the release tests carried out in PBS pH 7.4 revealed noticeably fast release (Table 1, entry 9). Compared to unprocessed vitamin E and vitamin E/aerogel physical mixtures that required 20 h in achieving 100% dissolution, vitamin E formulated in aerogels completed the dissolution in 75 min. In parallel, unprocessed vitamin K3 and its mixture with aerogels required 5 h to complete the dissolution, while vitamin K3-loaded aerogels provided completed dissolution in 80 min [106]. Taking into account the recommended dietary allowance (RDA) of vitamin E (15 mg) and vitamin K3 (0.1 mg), tablets containing 100 mg vitamin *E*-loaded aerogels and 1 mg vitamin K3-loaded aerogels could fulfil the daily needs of both vitamins.

Formulation of hydrophobic drugs into hydrophilic aerogels while still preserving the crystalline structure of the drug may be also feasible. Compared to amorphization reported above, formulation of crystalline forms has the advantage of improved stability [107]. Carbon aerogels have been designed to promote the π-π interactions with lipophilic drugs such as coenzyme Q10. Functionalization of the carbon aerogels with graphene oxide has been shown to enhance the rate and the amount of drug loaded (up to 0.05 mg/mg) when soaked in a drug solution in acetonitrile. The aerogels were air-dried at room temperature. Coenzyme Q10 was shown to be crystalline but the XRD pattern was different from that of the bulk drug, which has been explained by the confining effect that the aerogel pores may have on the crystal growth [108]. The effects on drug release are still to be elucidated.

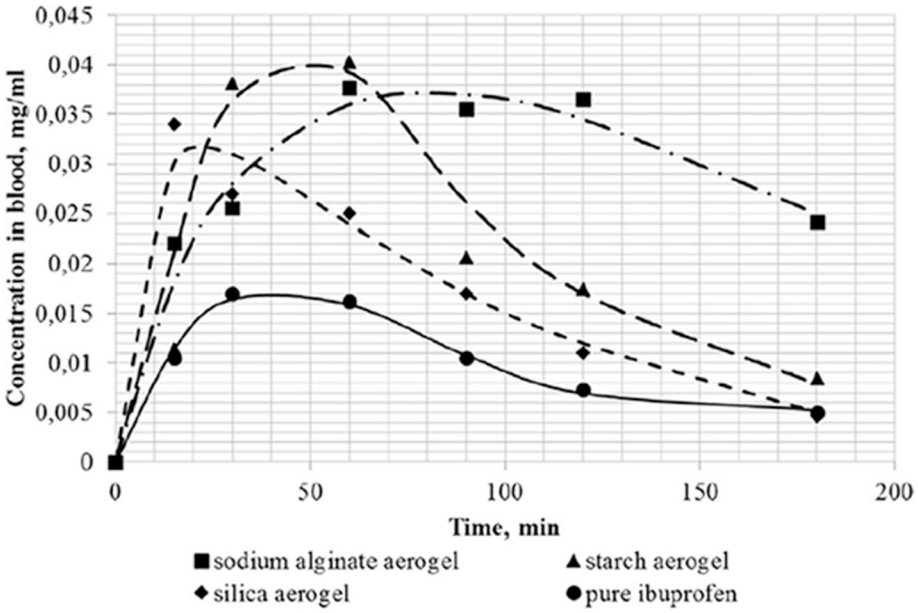


Fig. 9. Blood levels of ibuprofen after oral administration to Wistar rats of the same drug dose as oral dispersions of drug-loaded aerogels or unprocessed free drug. Reprinted from Lovskaya et al. [103] with permission from Elsevier.

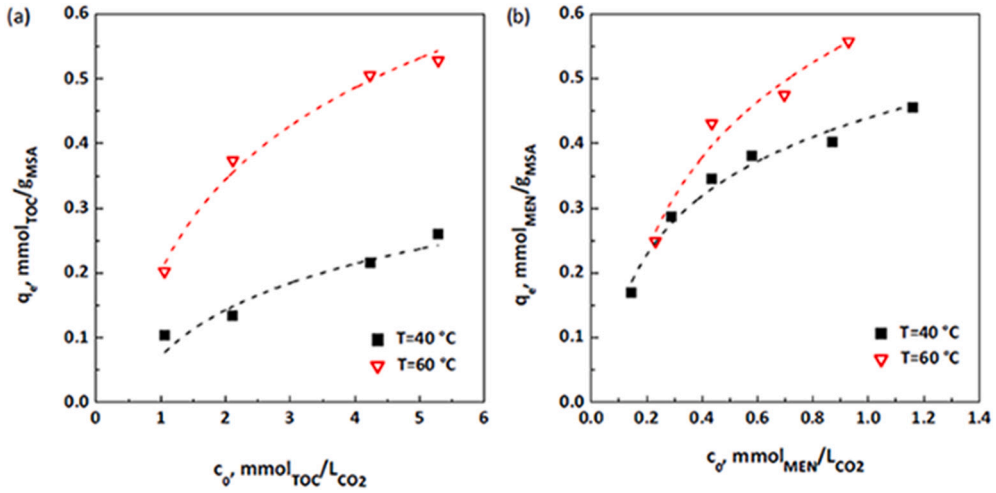


Fig. 10. Adsorption isotherms of vitamin E (α-tocopherol, TOC) and vitamin K3 (menadione, MEN) into maize starch aerogels (MSA) at 15 MPa and 40 or 60 °C after 48 h exposition. Reprinted from De Marco et al. [106] with permission from Elsevier.

3.2. Aerogels for sustained and stimuli-responsive release

Polymer-based aerogels are gaining increasing interest when searching for sustained oral release. The work in the field is still incipient and many unanswered questions remain. For example, most reports on aerogels for sustained release did not consider the stability of the aerogels in the presence of natural surfactants and human and bacteria enzymes typical of the small and large intestine. The manufacture of aerogel-based dosage forms (e.g., suspension, capsule, and tablet) while keeping aerogels integrity is another issue to be investigated. Nevertheless, the already available information points out some interesting performances of the aerogels as evidenced in the next lines below. Table 2 summarizes relevant examples of the interest of polymeric aerogels as components of sustained and stimuli-responsive release oral dosage form.

Starch and alginate aerogels either as monoliths or microspheres were one of the first investigated polysaccharide-based aerogels for drug delivery [35]. Starch aerogels from potato and Eurylon7 amylomaize were evaluated for the encapsulation of ibuprofen and paracetamol. Different loading protocols were followed considering the solubility of each drug: ibuprofen was loaded by $scCO_2$ impregnation of the preformed aerogel (Table 2, entry 1), while paracetamol was loaded through solvent exchange in drug-saturated ethanol before $scCO_2$ drying [109] (Table 2, entry 2). Eurylon7 starch aerogel loaded higher amounts of ibuprofen (22 vs. 10 wt%) and paracetamol (25 vs. 10 wt%) than potato starch aerogel, which may be related to the higher surface area of the former (90.3 vs. 72.5 m^2/g). Paracetamol was partially crystalline and its release in PBS pH 7.2 was completed in 2 h, which was slightly slower than unprocessed crystalline paracetamol. Differently, the ibuprofen release was sustained for more than 10 h despite being adsorbed as amorphous solid. Eurylon7 starch aerogel collapsed and disintegrated in contact with the release medium and released >60% in 4 h. Potato starch aerogel released less than 40% in the same time frame because of the higher stability of this aerogel in water [109]. Corn and pea starch aerogel microspheres obtained through the combination of emulsion-gelation and supercritical drying were investigated as ketoprofen carriers loaded by supercritical impregnation [110]. As in the case of silica aerogels, the loaded drug (11.5 wt%) did not display crystalline peaks, but the loading was one-order of magnitude larger and the release was more sustained from the starch aerogels. Ketoprofen release rate was slower than the dissolution rate of the crystalline drug in PBS pH 6.8, although the release was completed within 2 h (Table 2, entry 3).

Improved control of drug release was recorded for hybrid aerogels of multiwalled carbon nanotubes (CNTs) and konjac glucomannan and processed using freeze-drying. The aerogels were soaked in a 5-fluorouracil aqueous solution [111] (Table 2, entry 4). Konjac glucomannan aerogels without CNTs showed burst release, with most drug released in less than 2 h, regardless of the pH of the medium. An increase in the CNT content attenuated the burst effect and prolonged the release for more than 11 h due to strong drug-CNT hydrogen bonding [111]. Porosity and pore features of the aerogels were only qualitatively described, which makes comparisons with other aerogels difficult. Mesoporous carbon aerogels have shown remarkable capability to load drugs by soaking in drug solutions prepared in ethanol, as also demonstrated for ibuprofen [112]. Carbon aerogel monoliths of mean pore size 10 nm and 20 nm loaded 18.2 and 22.9 wt% ibuprofen, respectively, showed excellent compatibility with intestinal cells in vitro, and sustained drug release in both fasted and fed intestinal simulated fluids for several hours (Table 2, entry 5).

Barley and yeast β-glucan aerogels have been shown suitable to host relatively high amounts of the NSAID acetylsalicylic acid and to sustain its release. These two types of β-glucan significantly differ in chain structure and gelling capability. Barley glucan, a (1–3, 1–4)-β-glucan, is water soluble and requires a minimum concentration of 4 wt% to form gels upon cooling. Conversely, yeast glucan, a (1–3, 1–6)-β-glucan, is not soluble in water and requires only 2.5 wt% to form heat-induced gels. The respective alcogels were processed with $scCO_2$ in the presence of acetylsalicylic acid for drug adsorption and drying in one step [43]. Barley glucan aerogels had larger surface area (189 vs. 173 m^2/g), pore volume (0.713 vs. 0.563 cm^3/g), mean pore size (15.8 vs. 13.7 nm), and bulk density (69 vs. 35 Kg/m^3), but lower capability to uptake water (800 vs. 1400 wt%). The amount of acetylsalicylic acid notably depended on the conditions of supercritical processing but ranged between 8 and 15 wt% for all aerogels. No data about crystallinity was reported. Drug release tests carried out in PBS pH 7.4 at 37 °C evidenced remarkable differences between both glucan aerogels (Table 2, entry 6). Barley glucan aerogel showed 3 h lag time followed by an exponential increase in the release rate in the next 3 h and then, the release rate slowed down. Yeast glucan aerogel released 20% of the loaded drug in the first 2 h, followed by sustained release along 24 h. The higher capability of yeast glucan aerogels to swell in the aqueous medium without dissolution has been pointed out as the reason of the differences in drug release rate [43]. The delayed release observed for barley glucan aerogel proves that the drug was efficiently adsorbed inside the aerogel and not deposited on the surface, and that the release requires the previous swelling of the skeleton (wetting and relaxation of the chains). Thus, a combined contribution of matrix swelling and drug diffusion

Table 2
Examples of aerogels suitable for oral sustained release or stimuli-responsive release reported in the last decade.

Entry	Aerogel composition	Drug	Loading method	Release medium and outcomes	Reference
1	Potato starch and Eurylon 7 starch	Ibuprofen	$scCO_2$ impregnation of preformed aerogel	Buffer pH 7.2. Compared to crystalline ibuprofen, potato starch aerogels showed slower release rate (<50% in 6 h)	[109]
2	Potato starch and Eurylon 7 starch	Paracetamol	Solvent exchange in drug-saturated ethanol before $scCO_2$ drying	Buffer pH 7.2. 100% released in 2 h	[109]
3	Corn and pea starch	Ketoprofen	$scCO_2$ impregnation of preformed aerogel microspheres	Buffer pH 6.8; ~50% released in the first 1 h followed by 24 h sustained release	[110]
4	Multiwalled carbon nanotubes (CNTs) and konjac glucomann	5-fluorouracil	Soaking in a drug solution	Buffers pH 1.2 and 6.8. Sustained release for more than 11 h.	[111]
5	Carbon	Ibuprofen	Soaking in a drug solution	Fasted and fed intestinal simulated fluids. Less than 50% released after 2 h.	[112]
6	Barley glucan and yeast glucan	Acetylsalicylic acid	Simultaneous drug impregnation and supercritical drying.	Buffer pH 7.4. Barley glucan aerogel showed 3 h lag time followed by an exponential increase in release rate. Yeast glucan aerogel released 20% drug in the first 2 h followed by sustained release along 24 h	[43]
7	Cellulose nanofiber	Bendamustine hydrochloride	Soaking in a drug solution, and freeze-drying	Buffers pH 1.2 and 7.4. Sustained release for 24 h.	[113]
8	Cellulose nanofiber	Beclomethasone dipropionate	Drug nanoparticles dispersed with the nanofibers and freeze-dried	The aerogels were conditioned in gelatin capsules (size 0) and placed in 40 mL of 0.3% SDS. Aerogels made from bacterial cellulose, quince seed and oxidized birch cellulose sustained drug release for more than 10 h.	[20]
9	Alginate cross-linked with Ca^{2+}	Ketoprofen	$scCO_2$ impregnation	Buffers pH 1.2 and 6.8. Sustained release for more than 6 h.	[52]
10	Alginate, pectin and pectin-alginate cross-linked with Zn^{2+}	Diclofenac	Drug added to the polysaccharide dispersion	Buffers pH 1.2 and 6.8. Sustained release for more than 6 h.	[114]
11	Alginate cross-liked with Fe^{3+}	Ibuprofen	$scCO_2$ impregnation of the aerogels with ibuprofen w/o ascorbic acid	Buffers pH 2.2 and 7.4. Release faster in pH 7.4 due to erosion of aerogels. The release can be accelerated incorporating ascorbic acid into aerogels, which reduces Fe^{3+} to Fe^{2+}upon hydration.	[115]
12	High-methoxyl pectin	Nifedipine	Soaking in ethanol phase or $scCO_2$ impregnation	Buffers pH 1.2 and 6.8. Minor release at gastric pH, prolonged release at pH 6.8 for more than 6 h.	[116]
13	Guar and xantham gum	Nifedipine	Soaking in ethanol phase	Buffers pH 1.2 and 6.8. Minor release at gastric pH, prolonged release at pH 6.8 for more than 12 days.	[117]
14	Apple pectin and citrus pectin	Theophylline, nicotinic acid	Drug added to pectin dispersion before Ca^{2+} cross-linking	Buffer pH 6.5. Citrus pectin aerogels prolonged drug release for 6 h, compared to less than 1 h from apple pectin aerogels.	[118]
15	Chitosan, carboxymethyl cellulose and graphene oxide	5-fluorouracil	Soaking in a drug solution in water followed by freeze-drying	Buffers pH 1.2, 5.5 and 7.4. Minor release at pH 1.2; faster release at pH $\geq$ 5.5.	[119]
16	Graphene oxide and vitamin C	Doxorubicin	Drug added during nanoparticles preparation	Buffers pH 5.4 and 7.4. Sustained but faster release at pH 5.4 than 7.4.	[120]
17	Silica	Paclitaxel	Soaking in drug solution and freeze-drying	Simulated gastric (pH 1.5) and intestinal (pH 6.5) fluids. After 15 days, aerogels released less than 10% at pH 1.5 and about 50% at pH 6.5.	[121]
18	Halloysite nanoclay	Ibuprofen and dexamethasone	Dual loading. Ibuprofen added before cross-linking; dexamethasone loaded by soaking	Buffers pH 1.2 and 7.4. Sustained release for 2 days. Minor effect of pH.	[122]
19	Alginate grafted NIPA; and NHMAM	Indomethacine	Drug added before freeze-drying	Buffers pH 2.1 and 7.4. Release rate sustained for several hours, but faster at pH 7.4 and 42 °C than at 25 °C.	[123]
20	Whey protein	Ketoprofen	$scCO_2$ impregnation	Buffers pH 1.2 and 6.8. Anomalous non-Fickian drug release, faster at pH 6.8 than at 1.2	[125]
21	Whey protein, egg white protein or sodium caseinate	Fish oil	$scCO_2$ impregnation	Saliva, gastric and intestinal mimicking media. Resistance against digestion and selective release in the intestine mimicking environment.	[126]

governed the release kinetics.

Cellulose nanofiber aerogels processed applying freeze-drying have been investigated as gastro-retentive formulations due to their floatability and mucoadhesive performances [113]. The nanofibers were loaded with the anti-cancer agent bendamustine hydrochloride (~19 wt %) by soaking in a drug solution and then freeze-dried using mannitol as cryoprotectant. Total floating time in HCl buffer pH 1.2 and PBS pH 7.4 was similar and close to 450 min. The nanofiber aerogels showed preferential swelling in PBS pH 7.4 (225%) than in buffer pH 1.2 (189%). Bendamustine release was sustained in both pH 1.2 (69% released in 24 h) and pH 7.4 (78% released in 24 h) (Table 2, entry 7). The release profiles fitted to the Korsmeyer-Peppas model with n values of 0.613, suggesting once again the combined contribution of drug diffusion and matrix swelling. Drug pharmacokinetics was evaluated in a Wistar rat model for pure drug solution and the drug-loaded aerogels after oral administration and compared to intravenous administration of the drug solution. Relevantly, the nanofiber aerogels provided 5.66-fold and 3.25-fold higher area-under-the-curve (AUC) than the intravenous injection and the oral solution, respectively (Fig. 11).

In a comparative study, cellulose nanofiber aerogels of different sources were evaluated regarding their capability to sustain the release of the steroid beclomethasone dipropionate [20] (Table 2, entry 8). Nanoparticles of this drug were coated with amphiphilic hydrophobin proteins and dispersed in the cellulose nanofibers before freeze-drying. Aerogels made from red pepper cellulose or microcrystalline cellulose released the drug very rapidly (60% in 5 min), while those prepared with bacterial cellulose, quince seed and oxidized birch cellulose provided sustained drug release (10% released in 10 min; prolonged release for 700 min) [20]. The differences in capability to regulate drug release clearly correlated with the strength of the interactions of the drug nanoparticles with the cellulose skeleton.

Alginate aerogels have shown by themselves certain pH-

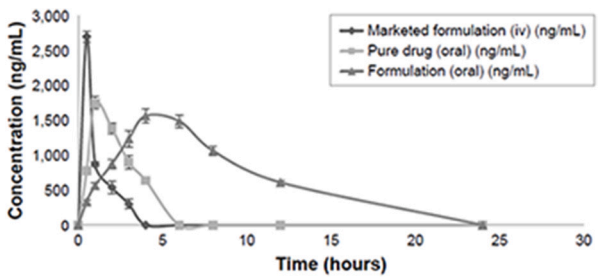


Fig. 11. Bendamustine blood levels after intravenous (iv) administration, oral administration of a drug solution and oral administration of drug-loaded cellulose nanofibers aerogels to Wistar rats. Reprinted from Bhandari et al. [113] with permission from Dove Medical Press.

responsiveness promoting the release of ketoprofen under acidic pH conditions despite that at such pH drug solubility is lower. Indeed, alginate aerogel microspheres prepared via emulsion-gelation (calcium crosslinking) and $scCO_2$ drying (116 μm; 524 m^2/g) and supercritically impregnated with ketoprofen (11.8 wt%) led to release profiles that fitted quite well to Korsmeyer-Peppas model (Table 2, entry 9). The exponent *n* was close to 0.4 at both pH values 1.2 and 6.8, but the release rate coefficient was higher at acidic pH (16.7 vs. 12.8 min^{-n}) [52]. This finding can be attributed to a weakening of the aerogels structure in HCl medium as the protons compete with the ionic crosslinking. Interestingly, the divalent counterion used to crosslink alginate seems to play a relevant role in the feasibility of obtaining sustained release formulations. Compared to the commonly used calcium ions, aerogels made of alginate, pectin and pectin-alginate crosslinked with zinc ions showed more prolonged release of diclofenac (Fig. 12) [114]. Differently to calcium crosslinked aerogels, those crosslinked with zinc loaded more drug, did not erode in simulated gastric fluid, and swelled more (58% vs. 34%) in PBS pH 6.8. Strontium cross-linked aerogels showed intermediate performance. At a similar concentration, zinc provided denser skeletons probably because these ions can interact with more binding sites in the alginate and pectin chains. Zinc-crosslinked pectin aerogels did not release diclofenac when immersed in simulated gastric fluid for 1 h and sustainedly released 80% of the cargo for 6 h when transferred to PBS pH 6.8, performing as an enteric formulation [114] (Table 2, entry 10). In another study, release profiles from alginate aerogels crosslinked with Fe(III) (~400 m^2/g) and impregnated with ibuprofen (35–40 wt%) were tuned by the addition of ascorbic acid (3.4–4.3 wt%) during $scCO_2$ impregnation (Table 2, entry 11). The aerogels showed an increase in release rate at pH 7.4 compared to pH 2.0, but the release rate was accelerated for aerogels containing ascorbic acid due to the capability of this reducing agent to transform Fe(III) into Fe(II), which weakens the crosslinking [115].

Pectin aerogels have also been tested for sustained but complete release of nifedipine, a BCS-Class II drug, after oral administration. High-methoxyl pectin aerogels (386 m^2/g surface area) were obtained by gelling of aqueous pectin dispersions (tablet-like shape) which were placed into contact with ethanol and then underwent $scCO_2$ drying. Nifedipine was loaded either during solvent exchange (in ethanol) or through supercritical adsorption. The loading was higher in the first option (22 vs. 13 wt%) but in both cases the drug remained amorphous [116]. Minor release was recorded after 2 h in gastric fluid due to small matrix swelling, but the release rate notably accelerated when the aerogels were transferred to a buffer medium of pH 6.8 (Table 2, entry 12) due to swelling and erosion of the aerogels. Supercritically loaded nifedipine was released in 6 h, while aerogels loaded by soaking in ethanol sustained the release for 10 h. Applying similar gelling and nifedipine loading in ethanol, low-methoxyl pectin, alginate, guar, and xanthan gum aerogels were generated [117]. All these aerogels exhibited pH-responsive erosion; they swelled in aqueous medium, but the swelling was faster, and the erosion was triggered when transferred from pH 1.2 to pH 6.8 medium. Nifedipine release from alginate and pectin aerogels was completed in 5 h at pH 6.8. Differently, nifedipine release from guar and xantham gums aerogels was prolonged for more than 12 days (Table 2, entry 13) due to the high stability in physiologically fluids, which may be useful for drug delivery using other administration routes. Also, the pectin source determined the capability of the aerogels to regulate drug release. Apple pectin aerogels (Ca(II) crosslinked) released the entire theophylline and nicotinic acid cargos within less than 1 h, while citrus pectin aerogels (Ca(II) crosslinked) sustained the release of any of these drugs for 6 h in buffer pH 6.5 [118] (Table 2, entry 14). Both apple and citrus pectin are low-methoxyl pectins but the small differences in degree of esterification (DE) and degree of amidation (DA) may interfere in the crosslinking process; citrus pectin with lower DE and higher DA was strongly and more uniformly crosslinked.

Aerogels can also be endowed with pH-responsive release properties by incorporating polycationic chitosan and polyanionic carboxymethyl cellulose. These two polysaccharides were combined with graphene oxide, crosslinked with Ca(II) ions, and freeze-dried to produce hybrid aerogel microspheres [119]. The anticancer agent 5-fluorouracil was loaded by soaking the aerogel in a drug solution followed by freeze-drying (Table 2, entry 15). The amounts released after 10 h at pH 1.2, 5.5 and 7.4 were 26, 51 and 68%, respectively, and the release kinetics could be described by Fickian diffusion [119]. Aiming to enhance the drug release under the acidic pH of solid tumors, graphene aerogel nanoparticles were prepared by reduction of graphene oxide sheets with vitamin C, sonication to break them into nanoparticles (180 nm), and loaded with doxorubicin [120]. In the first 24 h, the percentage of

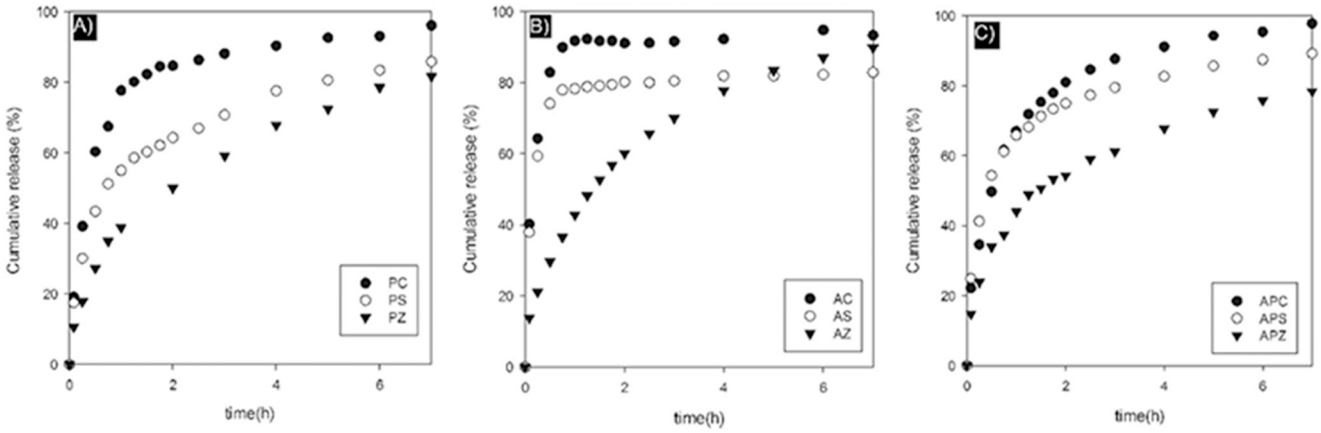


Fig. 12. Diclofenac release profiles in PBS pH 6.8 from (A) pectin, (B) alginate and (C) alginate-pectin aerogels crosslinked with calcium (PC, AC and APC, respectively), strontium (PS, AS and APS, respectively), or zinc (PZ, AZ and APZ, respectively). Reprinted from Tkalec et al. [114] with permission from Elsevier.

released doxorubicin was 40% at pH 7.4 and 60% at pH 5.4, but in this case, the faster release at pH 5.4 may be due to enhanced solubility of the encapsulated drug (Table 2, entry 16).

The benefits of aerogels as oral carriers of antitumor drugs that can attenuate the drawbacks of parenteral administration have been highlighted in a recent study. Silica aerogels were loaded with the poorly-water soluble anticancer agent paclitaxel by soaking them in a drug solution, freeze-drying and processing by spray-drying as spherical microparticles (2.56 μm) [121]. The aerogels remarkably increased the apparent drug (amorphous) solubility in water. In vitro release tests carried out in simulated gastric (pH 1.5) and intestinal (pH 6.5) fluids revealed that the drug can be selectively released in the intestine due to the pH-dependent release rate (Table 2, entry 17). In pH 6.5 medium, after a burst release of 20% in the first 24 h, the aerogels sustained the release for more than one month. Drug transport studies by using the Caco-2 cell monolayer model revealed that the aerogels increased drug permeability by 15- to 20-fold. The uptake of the paclitaxel-loaded silica aerogels into Caco-2 cells was increased 6- to 10-fold with respect to free drug. Enhanced uptake by tumor cells was also confirmed by using a breast cancer cell line (MCF7 cells). Moreover, the formulation into aerogels significantly decreased the viability of the tumor cells, showing lower inhibitory concentration 50 (IC_{50}). Moreover, intestinal absorption studies and blood levels in vivo revealed a 13-fold increase in relative oral bioavailability of the drug formulated in the aerogels compared to that of a commercially available formulation (Taxol). Real-time imaging evaluation of biodistribution of paclitaxel and antitumor efficacy in MCF7 subcutaneous xenografts confirmed the benefits of paclitaxel formulation in the oral aerogels compared to intravenous administration of the marketed formulation [121].

Aerogels prepared with halloysite nanoclay (HNT) have also showed capability to sustain the release of ibuprofen and dexamethasone at both gastric and intestinal pH, with slightly slower release rate at acidic pH [122]. First, HNT were loaded by soaking in ibuprofen solution and underwent polymerization and crosslinking with phenyl vinyl silicone oil to obtain microspheres that were finally loaded with dexamethasone also by soaking. The dually loaded HNT aerogels had specific surface area in the 176–138 m^2/g range with predominance of mesopores, sustained the release of both drugs for 48 h (Table 2, entry 18) and exhibited good compatibility with intestinal epithelial cells [122].

Dually temperature- and pH-responsive aerogels have been prepared using alginate grafted with PNIPAM (temperature-responsive block) and poly(*N*-hydroxymethylacrylamide) (PNHMAM, hydrophilic block). Indomethacin was added to the copolymer solution and then, the gels were freeze-dried [123]. Drug release was investigated at pH 2.1 and 7.4 and at 25 and 42 °C. Indomethacin release occurred faster at pH 7.4 according to the drug pH-dependent solubility profile (Table 2, entry 19). An increase in temperature from 25 to 42 °C notably accelerated further the release rate due to a squeezing effect as the aerogel network shrinks (Fig. 13). Other authors reported on temperature-sensitive aerogels from other sources such as cellulose and its derivatives [67,124].

Heat-denatured protein aerogels have demonstrated higher stability against disintegration in gastric and intestinal media compared to silica and polysaccharide aerogels. Whey protein, egg white protein or sodium caseinate have been shown suitable to prepare aerogels by solvent exchange and $scCO_2$ drying. Whey protein aerogels loaded with ketoprofen by supercritical impregnation showed a controlled and pH-dependent drug release at pH 1.2 and pH 6.8. Interestingly, the pH conditions used in the gelation process largely influenced the ketoprofen release profiles [125] (Table 2, entry 20). Protein aerogels supercritically impregnated with fish oil were subjected to digestion mimicking saliva, gastric and intestinal environments. Whey protein and sodium caseinate aerogels released the oil selectively in the intestinal environment (Table 2, entry 21). Egg white protein aerogels showed incomplete release due to an excessive resistance against enzymatic degradation [126]. Although not tested yet, the resistance to peptide digestion and the intestine-selective release of these heat-denatured proteins may open novel ways for the delivery of labile therapeutic molecules, such as peptides and proteins.

3.3. Coated and core-shell aerogels

As described above, non-functionalized silica aerogels commonly display immediate release because of the adsorption of the drug in the amorphous state on a skeleton that exposes an extraordinarily large surface area in contact with the physiological fluids. In addition to functionalization with hydrophobic moieties, coating of aerogels and preparation of core-shell architectures is being intensively investigated to regulate drug release. For instance, aerogel-hydrogel composite structures have been proposed to regulate ketoprofen release from silica aerogels [127]. The photoinitiator eosin was added to the alcogels during aging. Then, the alcogels underwent supercritical drying, optionally hydrophobic modification, and finally supercritical impregnation of ketoprofen. Hydrophilic and hydrophobic silica aerogels were coated with poly(ethylene glycol) (PEG) hydrogel via surface-initiated photopolymerization of the diacrylate monomer (MW 575 *Da*). Hydrophilic aerogels coated with thick PEG layers prolonged drug release in 0.1 N HCl medium for several days in a similar way as the non-coated hydrophobic aerogels. Ketoprofen diffusion coefficients were calculated to be $13.8{\cdot}10^{-6}$, $9.82{\cdot}10^{-6}$, $1.84{\cdot}10^{-6}$, $4.03{\cdot}10^{-6}$, and $0.32{\cdot}10^{-6}$ cm^2/min when delivered from hydrophilic, mid hydrophobic (66° water contact angle), strong hydrophobic (128°), PEG (15%)-coated hydrophilic and PEG (30%)-coated hydrophilic aerogels, respectively.

The interest in coatings to regulate drug release has also been explored for hybrid silica/alginate aerogels. The aerogels (900 m^2/g; 282 μm particle size) were prepared using an emulsification-internal setting protocol. Three different coatings were tested: alginate-hydroxypropyl methylcellulose (HPMC), silica-HPMC, and hydrophobic silica [128]. The beads (as hydrogels or alcogels) were dispersed in the coating aqueous solution and then mixed with an oily phase to obtain a water-in-oil emulsion (Fig. 14A). After aging, the coated hybrid beads were recovered, solvent exchanged and loaded with ketoprofen using supercritical processing. Interestingly, the presence of HPMC in the coatings notably enhanced drug deposition from 0.024 g/g in uncoated aerogels to 0.104 g/g in alginate-HPMC and 0.076 g/g in silica-HPMC coated ones. Aerogels with hydrophobic silica coating had a drug content of 0.045 g/g (4.5 wt%). Release tests carried out at pH 1.2

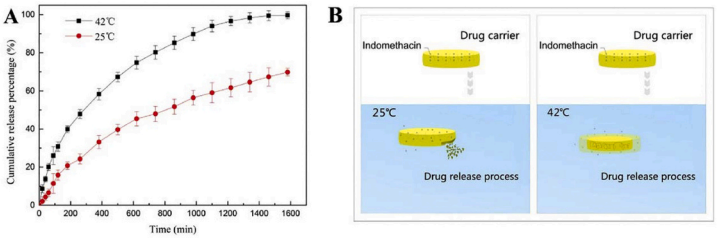


Fig. 13. (A) Indomethacin release profile from aerogels of alginate grafted with P(NIPAM-co-NHMAM) blocks recorded in buffer pH 7.4 at 25 and 42 °C and (B) sketch depicting the shrinking of the aerogels with the increase in temperature. Reprinted from Shao et al. [123] with permission from Elsevier.

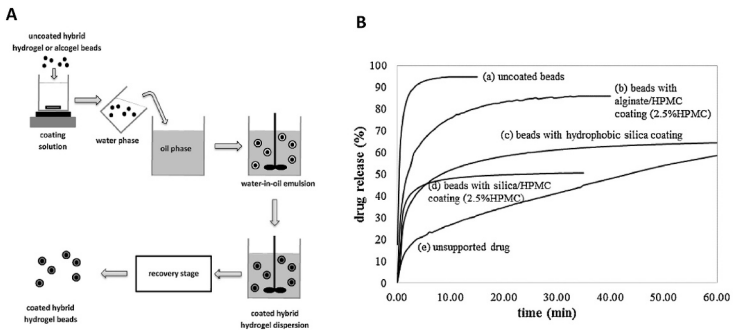


Fig. 14. (A) Scheme of the protocol followed to coat the hybrid beads before forming the aerogels, and (B) ketoprofen release profiles at pH 1.2 from the coated hybrid aerogels. Reprinted from Bugnone et al. [128] with permission of Elsevier.

indicated a very fast drug release from the uncoated hybrid aerogels (as expected) and slower release rate from the coated counterparts, particularly those coated with hydrophobic silica or silica/HPMC mixture (Fig. 14B). These latter coatings were more stable against disintegration in the acid medium. Nevertheless, the drug was still released faster than the dissolution rate of the unprocessed crystalline drug.

The effects of Eudragit® L (Pharma-grade copolymer of methacrylic acid and ethyl acrylate) coating on ibuprofen-loaded silica aerogels (1100 m^2/g; 200 μm-2 mm particle size) were investigated to obtain enteric formulations [21]. The content in supercritically adsorbed ibuprofen was 29 wt%. The loaded silica aerogels were first surface coated in a spouted bed with molten PEG2000 to protect the particles from the aqueous suspension of Eudragit® L also containing plasticizers. Direct exposition of the aerogels to the Eudragit® L suspension was shown to shrink the aerogels destroying the porous structure. Release tests carried out in 0.1 M HCl revealed that less than 20% of the loaded drug was released in 2 h (Fig. 15). The change to PBS pH 7.2 medium triggered the complete release of ibuprofen in less than 10 min. Although ibuprofen solubility is pH-dependent, the coating further contributed to prevent drug release at acidic pH. Moreover, a similar coating technology with Eudragit® L 30 D-55 applied to alginate-starch aerogels demonstrated the usefulness of the coating to preserve the aerogel structure during storage in environments of high relative humidity [129]. Overall, these results showed the feasibility of adapting a coating technology well-established in the pharmaceutical industry to the processing of drug-loaded aerogels.

Coating of triflusal-loaded silica and magnetite-silica aerogel particles with Eudragit® RL 100 has been also tested by using compressed CO_2-induced polymer precipitation. The aerogel particles were dispersed in a Eudragit® RL 100 solution in an organic solvent. The addition of CO_2 decreased the polymer solubility and provoked the precipitation on the surface of the particles, forming aggregates of aerogel nanoparticles. The coating notably improved drug stability during storage and provided sustained release for several hours in acidic medium (HCl) [130].

Recently, enzyme-responsive hybrid aerogels have been designed for selective drug release at colon. Silica aerogels were soaked in 5-fluorouracil solution and coated with dextran previous activation with glutaraldehyde of silica particles. Alternatively, the drug-loaded silica particles were directly coated with dextran aldehyde. The drug was in crystalline form and the uncoated aerogels released 78.4% and 86.4% after 4 h in simulated gastric and intestinal fluids in the absence of enzymes. The coatings slowed down the release to 1.3% and 3.5% released in the same time frame. Differently, in a release medium mimicking colon tumor environment (2 U dextranase/mL in acetate buffer pH 5.5) the aerogels coated with dextran or with dextran aldehyde increased the drug released to 24% and 13.4%, respectively. No changes were observed for non-coated silica aerogels. Relevantly, the coated aerogels without 5-fluorouracil were not toxic for Caco-2 cells, but once loaded with the drug the viability of these tumor cells decreased significantly, indicating the cytotoxic effect of the anticancer drug [131].

The multi-steps and long time processing involved in the coatings could be notably simplified by combination of co-axial prilling and supercritical drying. *Co*-axial prilling allows preparing core-shell or multilayered microgels in one step, with drugs in different layers. Subsequent drying with $scCO_2$ has been demonstrated to be a robust procedure to prepare core-shell aerogels with capability to regulate drug release profiles [132].

4. Aerogels for topical and transdermal administration

Delivery of drugs to and through the skin has traditionally been a subject of attention because of the inherent advantages of topical and transdermal routes to treat local and systemic diseases. Direct topical drug administration to the skin has the benefits of allowing for local treatment of pathologies that are not easily addressed through a systemic route, e.g., inflammation, bacteria and fungi infections and certain skin tumors. Drug administration through the skin (transdermal

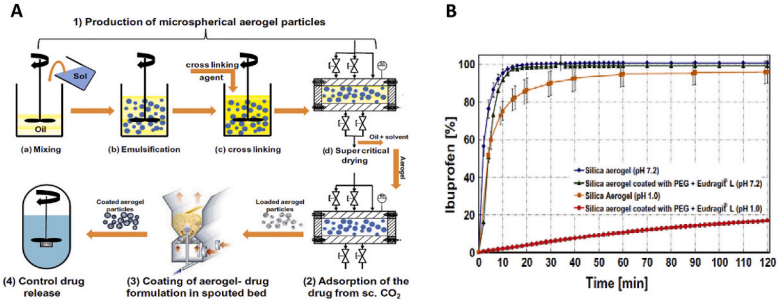


Fig. 15. (A) Scheme of the protocol followed to prepare silica aerogels and subsequent coating with stimuli-responsive polymers in a spouted bed, and (B) release profiles of ibuprofen from silica aerogels and Eudragit L-coated silica aerogels when placed in 0.1 M HCl (pH 1.0) or phosphate buffer pH 7.2 at 37 °C. Reprinted from Alnaief et al. [21] with permission from Elsevier.

delivery) has the advantage of avoiding liver first-pass metabolism, increasing systemic drug bioavailability, by using dosage forms that can be conveniently designed for prolonged delivery. Transdermal formulations combine the maintenance of drugs levels in blood without fluctuations and an excellent patient compliance. In addition, the treatment can be interrupted at any time. The main challenge for skin and transdermal formulations is the overcoming of the epithelium barrier (especially of the dense stratum corneum), which restricts these routes to potent small-molecule drugs. Gels are been positioned as excellent platforms to address some of these limitations thanks to the design of an ample variety of hydrogels, organogels, emulgels and more recently aerogels [133].

In a pioneering study, silica aerogels loaded with dithranol demonstrated enhanced drug penetration into human stratum corneum [25]. Dithranol is used in the management of psoriasis but requires discontinuous application to avoid skin discoloration and it is quite unstable. Therefore, an optimal formulation should provide fast therapeutic levels in deep epidermal regions. The silica aerogels were supercritically impregnated with dithranol (5 wt%) and then, dispersed in hydrophilic, lipophilic and PEG ointments. Free drug was similarly dispersed and the final drug concentration in the formulations varied between 0.5 and 1 wt %. First screening of drug permeability was carried out by using artificial membranes that mimic the stratum corneum (dodecanol collodion membrane and Nephrophan® membrane). Although crystalline dithranol is soluble in a lipophilic ointment, the addition of water or drug formulation into a hydrophilic ointment notably accelerated drug release from the silica aerogels due to the combined effect of the drug being in the amorphous state and the disintegration of the aerogel. Similarly, the highest permeability across the skin-mimicking membranes was also recorded for dithranol-loaded aerogels dispersed in the hydrophilic ointment. Compared to the standard formulation of dithranol in soft paraffin, dithranol-loaded aerogels dispersed in the hydrophilic ointment provided higher flux (0.61 vs 0.49 g/(m^2·h)) once applied on stratum corneum (Fig. 16) [25].

Strong research has been focused on development of antimicrobial aerogels [134]. Silica aerogels loaded with the hydrophobic antifungal fluconazole have been formulated in a sandwich-like multi-layer formulation, placing the aerogel particles in between a layer of poly (vinyl alcohol) (PVA) nanofibers and a PVA film [135]. PVA nanofibers containing the drug freely dispersed released the entire cargo within a few minutes [136]. Hydrophilic and hydrophobic silica aerogels loaded by soaking in a fluconazole solution in ethanol released the drug more controllably, according to a Fickian diffusion, but faster than the dissolution recorded for the non-processed crystalline drug. The multi-layer formulation provided structural support to the aerogel particles (PVA film) and a membrane (PVA nanofibers) to regulate the access of the release medium to the aerogels and the diffusion of the drug out. The drug-loaded silica aerogel particles that released more than 80% of the cargo in the first hour in contact with PBS, whereas the multi-layer composite sustained the release for more than 6 h following a non-Fickian mechanism (n =0.62–0.66) with the PVA swelling contributing to the control of drug release [135]. Relevantly, the antifungal activity against *Candida albicans* was preserved.

Chitosan aerogels functionalized with methacrylic acid and itaconic acid and prepared via supercritical drying were designed for pH-dependent release of thymol for antimicrobial topical application [137]. The aerogels were impregnated with thymol (up to 4.6 wt%) using $scCO_2$ and showed a high degree of swelling in aqueous medium, but the release profiles were not recorded.

Nanofibers endowed with the features of aerogels have also been tested regarding antimicrobial therapy. Nanofibers of methoxy PEG-polycaprolactone block copolymer (mPEG-PCL) were prepared via electrospinning of aqueous solutions followed by freeze-drying and crosslinking [138]. The aerogel fibers (230 m^2/g surface area; porosity >85%) behaved as water superabsorbents (25 g/g) and retained the mechanical properties and water sorption after 10 compression cycles. The fibers can be added with antimicrobial agents to be efficient against Gram-negative and Gram-positive bacteria in the treatment of skin wounds.

Composite aerogels made of graphene oxide and PVA have been designed to host hemostatic agents and to sorb water and blood without disintegration [139]. *Pais* grape extracts of seed and skin rich in proantocyanidins were mixed with graphene oxide and PVA and then freeze-dried. The composite aerogels sustained the release of the extract components for several hours and significantly shortened the coagulation time. The negative surface charge of graphene oxide contributed to the accumulation of blood cells on the surface of the aerogel and the

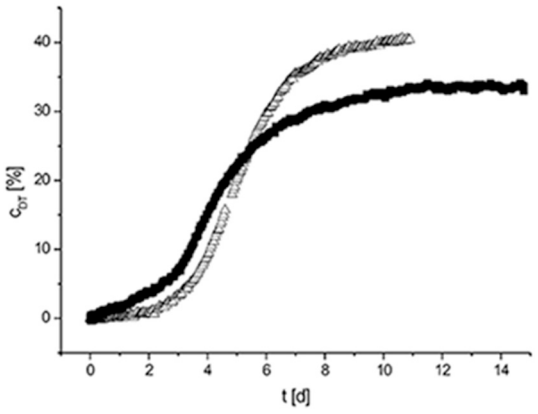


Fig. 16. Percentage of dithranol that permeated through stratum corneum towards the receptor chamber when applied as suspension in soft paraffin (black squares) and as drug-loaded silica aerogels dispersed in a hydrophilic ointment (open triangles). Reprinted from Guenther et al. [25] with permission from Elsevier.

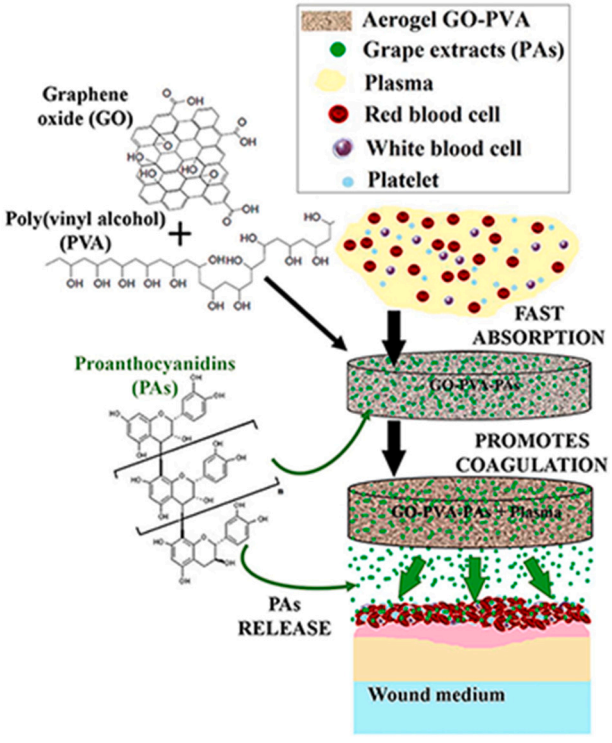


Fig. 17. Composite aerogels prepared by mixing graphene oxide, poly(vinyl alcohol) and extracts from *Pais* grape and obtained via freeze-drying showed rapid sorption of blood and short coagulation time. Reprinted with permission from Mellado et al. [139]. Copyright (2018) American Chemical Society.

stimulation of platelets, showing thrombogenic activity (Fig. 17). Similarly, hybrid composites of silica nanoparticles dispersed in hyperbranched networks of PVA and poly(acrylic acid) (PAA) and transformed into aerogels by freeze-drying, have been shown suitable to sustain the release of hydrophobic drugs. The aerogels showed excellent compatibility with fibroblasts, and increasing the PAA/PVA ratio, the release rate of dexamethasone was slower. Moreover, silica nanoparticles could be decorated with ammonium groups to exhibit bactericidal activity against common skin pathogens [140].

5. Aerogels for pulmonary and nasal administration

Most of the therapeutic proteins processed as inhalation powders and a growing percentage of the drug-loaded carriers for pulmonary administration are already prepared by using supercritical fluids [50]. As outlined above, $scCO_2$ allows the processing at near ambient temperature, which is especially favorable for labile therapeutic molecules. Moreover, the feasibility of tuning sizes and compositions and the excellent aerodynamic properties of the obtained particles (either drug-loaded or carrier-free) have pointed out supercritical fluid particle design as a key tool for dry powder inhaler (DPI) formulations [141,142]. Moreover, vaccines based on immunogenic nanoparticles for mucosal (nasal) administration are already being developed using the supercritical fluid technology [143].

Aerogels still represent an incipient contribution to the field among the different particle types that can be obtained via the supercritical fluid technology for pulmonary and nasal delivery. So far, aerogels for pulmonary treatments can be classified in two groups: (i) aerogels intended for lung administration; and (ii) aerogels that sustainedly release volatile compounds to the air for subsequent inhalation.

Hybrid aerogels made of mixtures of alginates and other polysaccharides attract attention for mucosal delivery. Aerogel microparticles of alginate and low methoxyl pectin and kappa-carrageenan obtained via $scCO_2$ drying showed high surface area (up to 548 m^2/g) and mucoadhesive properties [144]. Ketoprofen was loaded via $scCO_2$ adsorption (17–22 wt%) and quercetin was loaded during solvent exchange and deposited via gas antisolvent precipitation (3.1–5.4 wt%). In both cases, the drugs were in the amorphous state on the aerogel skeleton, and the release was completed within less than 60 min in PBS pH 6.8. To improve biodegradability in the lungs, hybrid alginate-hyaluronic acid aerogel microspheres with suitable aerodynamic diameter of 5 μm (446–611 m^2/g surface area) were designed [27]. The aerogels were prepared via emulsion-gelation followed by $scCO_2$ drying, conditioned in capsules (10 mg) to be inserted in a DPI device, and successfully evaluated in an Andersen Cascade Impactor internally coated to mimic the humidity of the airways. No data on drug release has been reported yet.

The bronchodilator salbutamol sulfate has also been formulated in aerogels to be delivered to the lungs. Chitosan-based aerogels obtained via conventional dropping and ionic gelation in sodium tripolyphosphate (STPP) solution showed capability to prolong salbutamol release, but the aerodynamic properties were not evaluated [145]. Recently, aerogels with very precise particle size and very narrow particle size distribution have been obtained by combination of the inkjet printing and the supercritical fluid technologies (Fig. 18A). This 3D-printing technology was firstly applied to prepare microspheres of alginate by precise dropping of the polymer dispersion in a calcium chloride solution also containing salbutamol sulphate [26]. The aerogels had a drug content of ~3 wt%, in line with commercially available DPI formulations, and showed sustained drug release in PBS pH 7.4 (Fig. 18B). As a proof-of-concept, the inkjet-printed aerogels (8 mg) were loaded in a capsule (size 3) and fitted to an impactor. The drug-loaded aerogels had 4.0 ± 1.5 μm aerodynamic diameter and exhibited good flowability, with most drug retained in the stage corresponding to the bronchi and bronchioles regions [26].

Recently, alginate-chitosan aerogels have been tested as carriers of antitumor drug cisplatin for intratracheal administration [28]. The aerogel particles (0.4 μm) prepared by emulsion gelation (without using divalent salt ions) followed by $scCO_2$ drying, were impregnated with the cytotoxic agent cisplatin crystalline particles under supercritical conditions. The aerogels released 60% of the drug in 2 h in phosphate buffer pH 7.4 and sustained the release of the remaining amount for six more hours. In vivo tests were carried out dispersing the aerogel particles in a small volume of saline serum and administered near the bifurcation of the trachea. Acute toxicity tests revealed that the materials used to prepare the aerogels are non-toxic by themselves. Subacute repeated administration tests indicated that the cisplatin dose was better tolerated when encapsulated in the aerogels, decreasing untoward events and mortality compared to the treatment with the free drug. Further in vivo studies should be focused on evaluating the biodegradability of the aerogels in the lung and the optimization of the amount of the drug encapsulated [28,146].

Another material under investigation as carriers for lung delivery of small-molecule drugs and proteins is graphene aerogel, which has shown high encapsulation yield of the antioxidant protein catalase and sustained release [147], though their biocompatibility by this administration route has not been demonstrated yet.

Differently to the direct drug delivery to the lungs, aerogels may also be intended for the release of volatile compounds to the air from which the compounds can be inhaled for a variety of therapeutic purposes. This strategy avoids the contact of excipient components of the aerogels with the mucosa. For example, hydrophilic (0.105 g/cm^3 bulk density) and hydrophobic (0.121 g/cm^3 bulk density) silica aerogels have been evaluated for the temperature-induced release of 1-menthol and 2-methoxy pyrazine [148]. These volatile compounds were loaded in the aerogels via $scCO_2$ impregnation. Both compounds are highly soluble in $scCO_2$ but 1-menthol is solid at room temperature and 2-methoxy pyrazine is liquid, which implies that the later does not solidify in the pores. Unprocessed 1-menthol evaporated completely after 55 min at 60 °C, but once included in the hydrophilic aerogels (23.3 wt% load) the release started when temperature reached 200 °C and was completed at 400 °C due to the strong hydrogen bonding with the silica skeleton. Release from hydrophobic aerogels (7.2 wt%) was triggered at 150 °C. In the case of 2-methoxy pyrazine (9.8 wt% load in hydrophilic and 3.3 wt

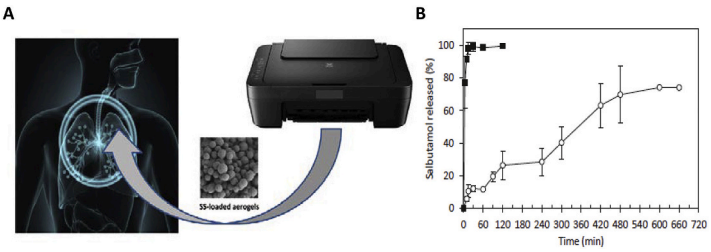


Fig. 18. (A) Application of the inkjet printing technology to the preparation of monodisperse alginate beads that were loaded with salbutamol sulphate, solvent exchanged and dried using $scCO_2$; and (B) Comparison of salbutamol sulphate release patterns from drug-loaded aerogels (open circles) and the unprocessed free drug solution (black squares). Reprinted from López-Iglesias et al. [26] with permission form Elsevier.

% in hydrophobic aerogels), fast release was recorded at 60 °C. Overall, the aerogels could be stored for several weeks at room temperature without loss of volatile compounds and should be moderately heated to trigger the release. Differently, aerogel microspheres from rice husk ash have shown remarkably large capability to adsorb eugenol (up to 8 g/g) and to release it to the air in a sustained way for 17 days at room temperature without need of heating [57].

Starch aerogels chemically crosslinked with trisodium citrate were tested for the release of trans-2-hexenal, a volatile antifungal agent. The aerogels were loaded by soaking in an aqueous drug solution and then surface-coated with Span 80 by spray coating. Aerogel formulations strongly retarded the release of the trans-2-hexenal at room temperature with respect to the free compound (1 h vs. 6–8 h for 100% release). The surface coating of the aerogels also delayed the antifungal activity against *Aspergilus parasiticus* inoculated in pistachio nuts reaching total inactivation after 19 h, in comparison to the 14 h for the uncoated aerogel counterpart [149]. In a similar context, aerogels loaded with hexanal (inhibitor of phospholipase D activity and of myco-toxins synthesis) were prepared by adding sunflower oil to galactoglucomannan and cellulose nanofibril hydrogel (cross-linked with ammonium zirconium carbonate) followed by freeze-drying [150]. The aerogels showed sustained release of hexanal for several weeks lipid oxidation pathway, with a rate regulated by the lipid oxidation pathway of the sunflower oil.

6. Emerging applications: gene therapy, theranostics and other biomedical applications

Combination of aerogel performances with novel materials (e.g. chips) and technologies (e.g. additive manufacturing) may further expand the scope of applications of aerogels in the drug delivery field.

Reports on aerogel-based implantable drug delivery systems for long-term release are still scarce. Biocompatibility of implants made of polyurea-crosslinked silica aerogels has been evaluated after subcutaneous and intramuscular implantation [151]. Preclinical evaluation through the monitoring of tissue damage, fibrosis and displacement of the implant for 20 months revealed that these aerogel-based implants can be considered as safe. No biodegradation was observed in vivo. Very relevantly, the implants inserted in the leg muscle did not move despite the absence of fixation (no suture) and unrestricted movement of the animal. This finding can be associated to the light weight (low density) typical of the aerogels. It should be noticed that the implants were manually shaped from monoliths, which may narrow the possibilities of fitting to the morphology demands of trocars used for the implantation and the tissue constrains. Additionally, a post-treatment with ethylene oxide was required to ensure sterility, which may be not compatible with some therapeutic substances. Advances in sterilization strategies that allow for aerogels processing and sterilization in one step may widen the therapeutic substances that can be included while shorten the processing time [19]. Interestingly, development of aerogel particles depots endowed with tumor-selective drug release was recently explored as coadjuvant therapy after tumor surgery or for the treatment of tumors that cannot be surgically resected [152]. Methotrexate was covalently conjugated to silica-gelatin aerogels through a labile bond that can be hydrolyzed by collagenases. In the absence of the enzyme the drug is not released. Differently, drug release rate is precisely regulated by the collagenase activity of the cells, which allows for differential drug accumulation in cancer and non-cancer cells.

A step forward in the development of implantable medicines is to adapt additive manufacturing technologies to aerogel materials. 3D-printing technologies may allow obtaining dosage forms with patient-personalized drugs, doses, and release profiles and with ad-hoc architectures to facilitate the administration through different routes [153]. Feasibility of producing spherical particles by inkjet printing [26] or complex objects with customizable pore structure through 3D microextrusion [154] has been demonstrated for silica and polysaccharide aerogels. In the case of 3D microextrusion of wet masses of cellulose nanocrystals, the aerogels were generated in a subsequent step involving freeze-drying. The obtained architectures showed physical properties suitable for the preparation of customizable scaffolds [154]. In the case of silica-based aerogels two different strategies have recently been explored for 3D printing: (i) 3D printing of silica alcogel precursor by irradiation of solutions of tetraethyl orthosilicate, diacrylates and photoinitiator (laser-induced 3D printing) [37], and (ii) 3D extrusion of preformed silica aerogels in the presence of silica nanoparticles, followed by gelling in ammonia atmosphere [10]. These two approaches are compatible with $scCO_2$ drying of the printed objects while maintaining excellent shape fidelity. The performances in the drug delivery field are still to be explored.

In addition to drugs, aerogels can incorporate enzymes and metals which opens the possibility of their use in theranostics (therapy + diagnostics). Only recently, silica aerogels have been adapted to act as supports of a variety of enzymes (glucose oxidase, acid phosphatase and xylanase) while preserving both the enzyme activity and the aerogel structure [155], which will open a wide range of novel applications. In the case of metals, a metallic precursor can be supercritically deposited into the aerogel structure or, alternatively, the preformed aerogel can be soaked in the metallic precursor. The subsequent reduction (chemical or thermal) of the precursor generates the metal nanoparticles in situ [156]. Compared to other technique to produce metal nanoparticles, the supercritical deposition has the advantages of precise control of size, shape, and more homogeneous distribution of the particles [157,158]. Bimetallic nanoparticles have been shown to preserve their properties without risk of aggregation when dispersed into aerogels. Detailed protocols for the preparation of metallic nanoparticles-aerogel composites have been recently revisited [159]. Bimetallic AuAg nanoparticles supported in aerogels have shown excellent performances for Surface Enhanced Raman Spectroscopy (SERS); the dispersion in aerogels remarkably improved the sensitiveness of a probe molecule [160]. Core-shell nanoparticles of Pd@Pt dispersed in PVA aerogel together with alcohol oxidase have been integrated in a portable (point-of-care) device for alcohol assay in saliva. Replacing the enzyme by glucose oxidase the same platform allows for quantification of glucose in blood [161].

Hybrid gold nanocrystals in graphene aerogels have demonstrated potential as sensors of circulating tumor DNA in human blood for patient stratification and monitoring of treatments [162]. If adapted to the sensing of specific biomarkers, the aerogels could be designed for feedback-regulated drug release. Combination of graphene and shape memory polymers has rendered aerogel frameworks that exhibit ultrafast response and large deformation under electrical stimulation, with potential for sensors and actuators [163]. Moreover, plasmonic metallic nanostructures can further expand the applications of aerogels in photothermal therapy. Irradiation of carbon aerogels with 808 nm laser has been shown suitable for ablation of osteosarcoma while serving as scaffold for bone regeneration [164]. This field is still very incipiently developed but a very appealing future can be predicted.

Feasibility of using aerogels as non-viral vectors for gene therapy is also under evaluation. Polyethylenimine (PEI), one of the most investigated condensing agents of gene material, can be grafted to cellulose nanofibril aerogels [165]. These biodegradable PEI-modified aerogels have shown high affinity for anionic drugs such as sodium salicylate, reaching loadings of 287 mg/g. Drug release was sensitive to both pH and temperature, being faster at pH 7.4 than pH 2.0 and at 37 °C than 20 °C. The grafting of PEI to silica particles has also been implemented [166]. DNA itself exhibits high affinity for pristine silica aerogels [167] and both DNA and small-interference RNA (siRNA) can be included into the mesopores [168,169] mainly through hydrogen bonding between the phosphate groups of the genetic material and the Si-OH groups of the aerogel. Reinforcement of the interactions with PEI may notably improve the performance of aerogels in the gene therapy field. In parallel, the capability of aerogels to capture nucleotide acids can be exploited also as sensors. Silica aerogels prepared in the presence of

ionic liquids have been shown also to immobilize oligonucleotides for selective recognition of complementary DNA targets [170].

7. Scale-up and life cycle assessment

The growing interest in aerogels and the wide range of applications in the pharmaceutical field lead to the need to hypothesize their manufacture on pilot and industrial scale. Indeed, despite the broad interest, aerogel production is generally treated considering the bench scale; however, some scientific papers on large-scale aerogel production have been published. It should also be considered that in the pharmaceutical field, aerogels are used for some applications in the form of microparticles of controlled size, and for some others as patches of known geometry. In the former case, continuous processes can be developed, whereas in the latter case the production of aerogels may require batch processes.

In general, a common approach for the scale-up of a process relies on the use of similarities of the processes carried out on different scales by means of dimensionless numbers, which characterize the process. A process is correctly scaled on a pilot or industrial scale if (i) it takes place in a plant with larger dimensions but the same geometry as the bench-scale plant; (ii) the dimensionless numbers characteristic of a given process, evaluated on the pilot and industrial scale plants, have the same numerical value as the dimensionless numbers calculated for the bench-scale plant [171].

Some papers related to the production of alginate aerogel obtained by emulsion gelation on a pilot scale have been published. For example, sodium alginate aerogel particles have been prepared by emulsion gelation and dripping methods followed by supercritical drying at various scales [172]. In the case of the lab-scale plant, an apparatus with a volume of 0.25 L was used, whereas in the pilot-scale plant the volume of the vessel was 2 L. Alginate aerogel microparticles were also produced using emulsification setups with different dimensions: a batch setup producing an emulsification volume of 130 mL, a semi-continuous set-up with a 2 L funnel, and a continuous setup fed by a mixture of oil and alginate solution from two 20 L vessels [173]. When microparticles or microemulsions have to be treated, the atomization step is crucial, because it affects the final particle size; therefore, the scale-up is generally performed taking constant the Reynolds number (*Re*) and the Ohnesorge number (Oh). *Re* is the well-known ratio of inertial forces to viscous forces, as expressed in Eq. (4)

$$Re = \frac{Dv\rho}{\mu} \tag{4}$$

whereas Oh is the ratio between the viscous forces and the surface tension, as presented in Eq. (5)

$$Oh = \frac{\mu}{\sqrt{\rho\sigma D}} \tag{5}$$

where D is the nozzle diameter, ρ and μ are the density and viscosity of the fluid, v is the velocity and σ is the surface tension.

Production of aerogels in the form of patches of a given geometry is intrinsically a batch process, and the process scale-up has been rarely performed. In these cases, quasi-continuous productions are developed considering two or three minibatches that operate alternately. The effect of the plant scale-up on the production of starch aerogel for drug delivery was studied from an environmental point of view [174]. Two different scales were considered for the supercritical drying: a bench-scale plant with a vessel volume equal to 0.5 L and a pilot scale plant with a vessel volume equal to 5.2 L. The environmental impacts on an industrial scale plant (vessel volume equal to 100 L) were also simulated. In order to quantify the environmental impacts of the aerogel production process, demonstrating that the scale-up significantly reduces the emissions, the impacts related to the process conducted on the bench-scale and on the pilot-scale plant were compared through a life cycle assessment (LCA) analysis. LCA is a recognized tool used to quantify the environmental impact of a product or a process throughout its life cycle, identifying the steps of the process that are critical from the environmental point of view. The chosen functional unit used to compare, from the environmental point of view, the production of starch aerogel at different scales was equal to 1 g of aerogel. The analysis allowed comparing the process conducted on different scales using, according to the IMPACT 2002+ method [174], fifteen midpoint indicators or four damage categories: human health, ecosystem quality, climate change and resources (Fig. 19).

Comparing the environmental impact related to the different damage categories, the scale-up from the bench-scale to the pilot-scale implied a reduction of the impact equal to 68% considering the human health, 72% considering both ecosystem quality and climate change and 74% considering the resources. From the simulation on the industrial scale plant, it is possible to hypothesize a reduction of the impact equal to 96% considering the ecosystem quality and to 95% considering human health, climate change and the resources.

More recently, the LCA of the impregnation of starch aerogel with alpha-tocopherol was performed considering the processing on industrial scale [175]. Two different $scCO_2$ based processes were considered. First, the supercritical drying in a 100 L vessel was used to obtain the starch aerogel from the alcogel, then vitamin E (alpha-tocopherol) was impregnated into the aerogel using a 20 L internal volume plant. All the emissions were reported to the chosen functional unit, which was a 120 mg starch aerogel tablet containing 15 mg of alpha-tocopherol (daily therapeutic dose).

The performed analysis showed that the stages most affecting the environmental categories were the agricultural stages, the supercritical drying to obtain the aerogel, and the supercritical impregnation. Some scenarios were proposed to minimize the impacts of these steps, which included the possibility of recycling part of the ethanol (used in the hydrogel-to-alcogel step) and of reducing the consumption due to the CO_2 condensation.

8. Conclusions and future perspectives

The unique features of aerogels open new avenues to address relevant drug formulation challenges and to design advanced drug delivery systems with novel performances. Poor drug solubility can be overcome by deposition on the aerogel skeleton of large amounts of drug in the amorphous state. The large surface area with an enormous interconnected pore network facilitates the contact with the aqueous milieu and the diffusion of the dissolved drug. Alternatively, the drug release patterns can be regulated through a variety of options like the combination of swellable/erodible skeleton components, the tuning of the intensity of the drug/skeleton interactions, the coating with membrane-like substances and the integration of stimuli-responsive components. Moreover, the large surface area, low density, and capability to uptake liquids, which are genuine properties of aerogels, expedite the direct application of aerogels through a variety of mucosal administration routes, particularly oral, pulmonary, nasal and topical. Current protocols to manufacture aerogels already allow the use of almost any organic or inorganic material as skeleton component and can be adapted to formulate drugs with quite different physicochemical features and stability. Versatility is also extensive to the final sizes and formats of aerogel formulations. Relevantly, so far toxicological studies pointed out aerogels as quite safe [176,177], but further in vivo studies are still required.

Analysis of the literature on aerogel production clearly shows that most of the published articles are related to bench-scale production. The growing interest in the application of aerogels in the pharmaceutical field prompts experimentation on a pilot scale as a first step towards aerogels' production at the industrial scale. Large-scale (industrial) production of aerogels also needs considering the environmental aspects related to the production itself. LCA analysis enables the quantification

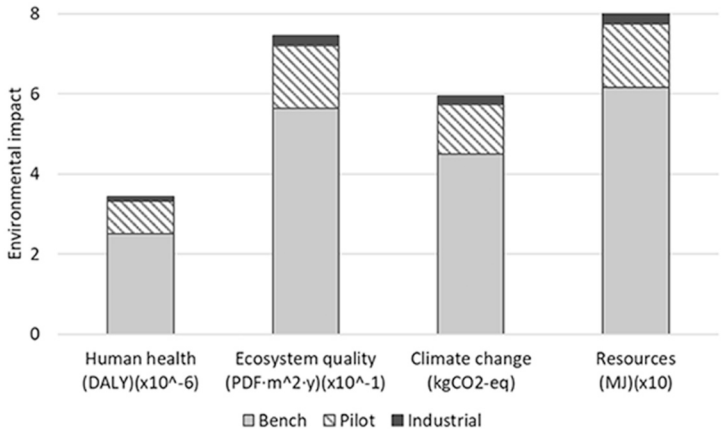


Fig. 19. Damage categories for aerogel production of different scales. Adapted from De Marco et al. [174] with permission from Springer Nature.

of specific impacts of the various production stages involved to identify the most impacting phases and propose strategies to minimize their impact.

Considering the interest in the use of aerogels in the pharmaceutical field and provided that the operating conditions can be optimized from the point of view of minimizing the environmental impact of the processes, these materials seem ready to be produced on an industrial scale. Next steps should focus on how drug-loaded aerogels can be transformed into true medicines. Namely, the possibilities of obtaining tablets, capsules, ointments, inhalation powders or injectable formulations, among others, while preserving the unique properties of aerogels are still to be explored.

Acknowledgements

Work carried out in the frame of COST Action CA18125 “Advanced Engineering and Research of aeroGels for Environment and Life Sciences” (AERoGELS), funded by the European Commission. This work was also supported by Xunta de Galicia [ED431C 2020/17], MCIUN [RTI2018-094131-A-I00], Agencia Estatal de Investigación [AEI], FEDER funds, and National Research, Development and Innovation Office, Hungarian Science Foundation [OTKA: FK_17-124571]. C.A. García-González acknowledges to MINECO for a Ramón y Cajal Fellowship [RYC2014-15239].

References

[1] A. Du, B. Zhou, Z. Zhang, J. Shen, A special material or a new state of matter: a review and reconsideration of the aerogel, Materials 6 (2013) 941–968.
[2] A. Zaman, F. Huang, M. Jiang, W. Wei, Z. Zhou, Preparation, properties, and applications of natural cellulosic aerogels: a review, EBE 1 (2020) 60–76.
[3] L. An, J. Wang, D. Petit, J.N. Armstrong, K. Hanson, J. Hamilton, M. Souza, D. Zhao, C. Li, Y. Liu, Y. Huang, Y. Hu, Z. Li, Z. Shao, A.O. Desjarlais, S. Ren, An all-ceramic, anisotropic, and flexible aerogel insulation material, Nano Lett. 20 (2020) 3828–3835.
[4] F. Deuber, S. Mousavi, L. Federer, C. Adlhart, et al., Adv. Mater. Interfaces 4 (2017), 1700065.
[5] F.J. Burpo, E.A. Nagelli, L.A. Morris, J.P. McClure, M.Y. Ryu, J.L. Palmer, Direct solution-based reduction synthesis of Au, Pd, and Pt aerogels, J. Mater. Res. 32 (2017) 4153–4165.
[6] P. Herman, I. Fabian, J. Kalmar, Mesoporous silica–gelatin aerogels for the selective adsorption of aqueous Hg(II), ACS Appl, Nanostruct. Mater. 3 (2020) 195–206.
[7] E. Barrios, D. Fox, Y.Y.L. Sip, R. Catarata, J.E. Calderon, N. Azim, S. Afrin, Z. Y. Zhang, L. Zhai, Nanomaterials in advanced, high-performance aerogel composites: a review, Polymers 11 (2019) 726.
[8] Z. Liu, Y. Ran, J. Xi, J. Wang, Polymeric hybrid aerogels and their biomedical applications, Soft Matter 16 (2020) 9160–9175.
[9] Q. Zhang, F. Zhang, S.P. Medarametla, H. Li, C. Zhou, D. Lin, 3D printing of graphene aerogels, Small 12 (2016) 1702–1708.
[10] S. Zhao, G. Siqueira, S. Drdova, D. Norris, C. Ubert, A. Bonnin, S. Galmarini, M. Ganobjak, Z. Pan, S. Brunner, G. Nyström, J. Wang, M.M. Koebel, W.J. Malfait, Additive manufacturing of silica aerogels, Nature 584 (2020) 387–392.
[11] S. Zhao, W.J. Malfait, N. Guerrero-Alburquerque, M.M. Koebel, G. Nyström, Biopolymer aerogels and foams: chemistry, properties, and applications, Angew. Chem. Int. Ed. 57 (2018) 7580–7608.
[12] S. Wei, Y.C. Ching, C.H. Chuah, Synthesis of chitosan aerogels as promising carriers for drug delivery: a review, Carbohydr. Polym. 231 (2020) 115744.
[13] L.E. Nita, A. Ghilan, A.G. Rusu, I. Neamtu, A.P. Chiriac, New trends in bio-based aerogels, Pharmaceutics 12 (2020) 449.
[14] C.A. García-González, T. Budtova, L. Durães, C. Erkey, P. Del Gaudio, P. Gurikov, M. Koebel, F. Liebner, M. Neagu, I. Smirnova, An opinion paper on aerogels for biomedical and environmental applications, Molecules 24 (2019) 1815.
[15] H. Paukkonen, M. Kunnari, P. Lauren, T. Hakkarainen, V.V. Auvinen, T. Oksanen, R. Koivuniemi, M. Yliperttula, T. Laaksonen, Nanofibrillar cellulose hydrogels and reconstructed hydrogels as matrices for controlled drug release, Int. J. Pharm. 532 (2017) 269–280.
[16] A. Soleimani Dorcheh, M.H. Abbasi, Silica aerogel; synthesis, properties and characterization, J. Mater. Process. Technol. 199 (2008) 10–26.
[17] C. Vakifahmetoglu, D. Zeydanli, V.C. Ozalp, B.A. Borsa, G.D. Soraru, Hierarchically porous polymer derived ceramics: A promising platform for multidrug delivery systems. Mater, Design 140 (2018) 37–44.
[18] I. Pasquali, R. Bettini, Are pharmaceutics really going supercritical, Int. J.Pharm. 364 (2008) 176–187.
[19] N. Ribeiro, G.C. Soares, V. Santos-Rosales, A. Concheiro, C. Alvarez-Lorenzo, C. A. García-González, A.L. Oliveira, A new era for sterilization based on supercritical CO_2 technology, J Biomed Mater Res B Appl Biomater 108 (2020) 399–428.
[20] H. Valo, S. Arola, P. Laaksonen, M. Torkkeli, L. Peltonen, M.B. Linder, R. Serimaa, S. Kuga, J. Hirvonen, T. Laaksonen, Drug release from nanoparticles embedded in four different nanofibrillar cellulose aerogels, Eur. J. Pharm. Sci. 50 (2013) 69–77.
[21] M. Alnaief, S. Antonyuk, C.M. Hentzschel, C.S. Leopold, S. Heinrich, I. Smirnova, A novel process for coating of silica aerogel microspheres for controlled drug release applications, Microporous Mesoporous Mater. 160 (2012) 167–173.
[22] Z. Ulker, C. Erkey, A novel hybrid material: an inorganic silica aerogel core encapsulated with a tunable organic alginate aerogel layer, RSC Adv. 4 (2014) 62362–62366.
[23] A. Veronovski, Ž. Knez, Z. Novak, Preparation of multi-membrane alginate aerogels used for drug delivery, J. Supercrit. Fluids 79 (2013) 209–215.
[24] C. López-Iglesias, J. Barros, I. Ardao, P. Gurikov, F.J. Monteiro, I. Smirnova, C. Alvarez-Lorenzo, C.A. García-González, Jet cutting technique for the production of chitosan aerogel microparticles loaded with vancomycin, Polymers 12 (2020) 273.
[25] U. Guenther, I. SmirnovaI, R.H.H. Neubert, Hydrophilic silica aerogels as dermal drug delivery systems-dithranol as a model drug, Eur. J. Pharm. Biopharm. 69 (2008) 935–942.
[26] C. López-Iglesias, A.M. Casielles, A. Altay, R. Bettini, C.A. Alvarez-Lorenzo, C. A. García-González, From the printer to the lungs: inkjet-printed aerogel particles for pulmonary delivery, Chem. Eng. J. 357 (2019) 559–566.
[27] T. Athamneh, A. Amin, E. Benke, R. Ambrus, C.S. Leopold, P. Gurikov, I. Smirnova, Alginate and hybrid alginate-hyaluronic acid aerogel microspheres as potential carrier for pulmonary drug delivery, J. Supercrit. Fluids 150 (2019) 49–55.
[28] M.M. Alsmadi, R.M. Obaidat, M. Alnaief, B.A. Albiss, N. Hailat, Development, in vitro characterization, and in vivo toxicity evaluation of chitosan-alginate nanoporous carriers loaded with cisplatin for lung cancer treatment, AAPS PharmSciTech 21 (2020) 191.
[29] V.S.S. Goncalves, A.A. Matias, J. Poejo, A.T. Serra, C.M.M. Duarte, Application of RPMI 2650 as a cell model to evaluate solid formulations for intranasal delivery of drugs, Int. J. Pharm. 51 (2016) 1–10.
[30] J. Yang, Y. Li, Y.Y. Zheng, Y.M. Xu, Z.K. Zheng, X.D. Chen, W. Liu, Versatile aerogels for sensors, Small 15 (2019) 1902826.

[31] L.P. Zheng, S.D. Zhang, Z.R. Ying, J.J. Liu, Y.H. Zhou, F. Chen, Engineering of aerogel-based biomaterials for biomedical applications, Int. J. Nanomedicine 15 (2020) 2363–2378.
[32] C.A. García-González, A. Concheiro, C. Alvarez-Lorenzo, Processing of materials for regenerative medicine using supercritical fluid technology, Bioconjug. Chem. 26 (2015) 1159–1171.
[33] C.A. García-González, L.A. Díaz-Gómez, A. Concheiro, C. Alvarez-Lorenzo, Patent survey on current applications of supercritical fluid technology in regenerative medicine, Recent Patents Nanomed. 5 (2015) 48–58.
[34] Z. Ulker, C. Erkey, An emerging platform for drug delivery: aerogel based systems, J. Control. Release 177 (2014) 51–63.
[35] C.A. García-González, M. Alnaief, I. Smirnova, Polysaccharide-based aerogels-Promising biodegradable carriers for drug delivery systems, Carbohydr. Polym. 86 (2011) 1425–1438.
[36] T.A. Esquivel-Castro, M.C. Ibarra-Alonso, J. Oliva, A. Martinez-Luevanos, Porous aerogel and core/shell nanoparticles for controlled drug delivery: a review, Mater. Sci. Eng. C Mater. Biol. Appl. 96 (2019) 915–940.
[37] S. Saeed, R.M. Al-Sobaihi, M.F. Bertino, L.S. White, K.M. Saoud, Laser induced instantaneous gelation: aerogels for 3D printing, J. Mater. Chem. A 3 (2015) 17606–17611.
[38] J. Stergar, U. Maver, Review of aerogel-based materials in biomedical applications, J. Solgel Sci. Technol. 77 (2016) 738–752.
[39] A. Veronovski, Z. Novak, Z. Knez, Synthesis and use of organic biodegradable aerogels as drug carriers, J. Biomater. Sci. Polym. Ed. 23 (2012) 873–886.
[40] Y.X. Wang, Z.Y. Kao, T. Zhang, Y.J. Zhang, L.L. Qin, Z.H. Zhang, B. Zhou, G. M. Wu, J. Shen, A. Du, Diffusion of resveratrol in silica alcogels, Molecules 24 (2019) 3931.
[41] Z. Ulker, C. Erkey, An advantageous technique to load drugs into aerogels: gas antisolvent crystallization inside the pores, J. Supercrit. Fluids 120 (2017) 310–319.
[42] M. Villegas, A.L. Oliveira, R.C. Bazito, P. Vidinha, Development of an integrated one-pot process for the production and impregnation of starch aerogels in supercritical carbon dioxide, J. Supercrit. Fluids 154 (2019) 104592.
[43] M. Salgado, F. Santos, R. Rodriguez-Rojo, R.L. Reis, A.R.C. Duarte, M.J. Cocero, Development of barley and yeast beta-glucan aerogels for drug delivery by supercritical fluids, J. CO2 Util. 22 (2017) 262–269.
[44] I. Smirnova, S. Suttiruengwong, M. Seiler, W. Arlt, Dissolution rate enhancement by adsorption of poorly soluble drugs on hydrophilic silica aerogels, Pharm. Dev. Technol. 9 (2004) 443–452.
[45] M.T. Falahati, S.M. Ghoreishi, Preparation of Balangu (*Lallemantia royleana*) seed mucilage aerogels loaded with paracetamol: evaluation of drug loading via response surface methodology, J. Supercrit. Fluids 150 (2019) 1–10.
[46] D.A.S. Agostinho, A.I. Paninho, T. Cordeiro, A.V.M. Nunes, I.M. Fonseca, C. Pereira, A. Matias, M.G. Ventura, Properties of κ-carrageenan aerogels prepared by using different dissolution media and its application as drug delivery systems, Mater. Chem. Phys. 253 (2020) 123290.
[47] US FDA, Sec. 184.1240 Carbon dioxide, Code of Federal Regulations, Title 21 vol. 3, 2019, https://www.accessdata.fda.gov/scripts/cdrh/cfdocs/cfcfr/CFRSearch.cfm?fr=184.1240. Accessed August 2020.
[48] A. Tabernero, E.M. Martín Del Valle, M.A. Galan, Supercritical fluids for pharmaceutical particle engineering: methods, basic fundamentals and modelling, Chem. Eng. Process. 60 (2012) 9–25.
[49] H. Weingärtner, E.U. Franck, Supercritical water as a solvent, Angew. Chem. Int. Ed. 44 (2005) 2672–2692.
[50] R.K. Kankala, Y.S. Zhang, S.B. Wang, C.H. Lee, A.Z. Chen, Supercritical fluid technology: an emphasis on drug delivery and related biomedical applications, Adv. Healthcare Mater. 6 (2017) 1700433.
[51] L. Padrela, M.A. Rodrigues, A. Duarte, A.M.A. Dias, M.E.M. Braga, H.C. de Sousa, Supercritical carbon dioxide-based technologies for the production of drug nanoparticles/nanocrystals – a comprehensive review, Adv. Drug Deliv. Rev. 131 (2018) 22–78.
[52] C.A. García-González, M. Jin, J. Gerth, C. Alvarez-Lorenzo, I. Smirnova, Polysaccharide-based aerogel microspheres for oral drug delivery, Carbohydr. Polym. 117 (2015) 797–806.
[53] P. Gurikov, I. Smirnova, Amorphization of drugs by adsorptive precipitation from supercritical solutions: a review, J. Supercrit. Fluids 132 (2018) 105–125.
[54] G. Caputo, M. Scognamiglio, I. De Marco, Nimesulide adsorbed on silica aerogel using supercritical carbon dioxide, Chem. Eng. Res. Design 90 (2012) 1082–1089.
[55] C.A. Lipinski, F. Lombardo, B.W. Dominy, P.J. Feeney, Experimental and computational approaches to estimate solubility and permeability in drug discovery and development settings, Adv. Drug Deliv. Rev. 46 (2001) 3–26.
[56] I. Medina, Determination of diffusion coefficients for supercritical fluids, J. Chromatogr. A 1250 (2012) 124–140.
[57] S.K. Rajanna, D. Kumar, M. Vinjamur, M. Mukhopadhyay, Silica aerogel microparticles from rice husk ash for drug delivery, Ind. Eng. Chem. Res. 54 (2015) 949–956.
[58] M. Mohammadian, T.S.J. Kashi, M. Erfan, F.P. Soorbaghi, Synthesis and characterization of silica aerogel as a promising drug carrier system, J. Drug Deliv. Sci. Technol. 44 (2018) 205–212.
[59] A.L. Ajiboye, V. Trivedi, J. Mitchell, Mesoporous silica particles as potential carriers for protein drug delivery: protein immobilization and the effect of displacer on γ-globulin release, Drug Dev. Ind. Pharm. 46 (2020) 576.
[60] M. Alnaief, I. Smirnova, Effect of surface functionalization of silica aerogel on their adsorptive and release properties, J. Non-Cryst. Solids 356 (2010) 1644–1649.
[61] N. Saad, M. Chaaban, D. Patra, A. Ghanem, H. El-Rassy, Molecularly imprinted phenyl-functionalized silica aerogels: selective adsorbents for methylxanthines and PAHs, Microporous Mesoporous Mater. 292 (2020) 109759.
[62] N. Kamaly, B. Yameen, J. Wu, O.C. Farokhzad, Degradable controlled-release polymers and polymeric nanoparticles: mechanisms of controlling drug release, Chem. Rev. 116 (2016) 2602–2663.
[63] J. Siepmann, F. Siepmann, Modeling of diffusion controlled drug delivery, J. Control. Release 161 (2012) 351–362.
[64] J. Siepmann, F. Siepmann, Mathematical modeling of drug dissolution, Int. J. Pharm. 453 (2013) 12–24.
[65] J. Kalmár, M. Kéri, Z. Erdei, I. Bányai, I. Lázár, G. Lente, I. Fábián, The pore network and the adsorption characteristics of mesoporous silica aerogel: adsorption kinetics on a timescale of seconds, RSC Adv. 5 (2015) 107237–107246.
[66] L. Janovák, Á. Turcsányi, É. Bozó, Á. Deák, L. Mérai, D. Sebők, Á. Juhász, E. Csapó, M.M. Abdelghafour, E. Farkas, I. Dékány, F. Bari, Preparation of novel tissue acidosis-responsive chitosan drug nanoparticles: characterization and in vitro release properties of Ca2+ channel blocker nimodipine drug molecules, Eur. J. Pharm. Sci. 123 (2018) 79–88.
[67] Z. Liu, S. Zhang, B. He, S. Wang, F. Kong, Temperature-responsive hydroxypropyl methylcellulose-N-isopropylacrylamide aerogels for drug delivery systems, Cellulose 27 (2020) 9493–9504.
[68] M. Pantic, G. Horvat, Z. Knez, Z. Novak, Preparation and characterization of chitosan-coated pectin aerogels: curcumin case study, Molecules 25 (2020) 1187.
[69] I. Lázár, A. Forgács, A. Horváth, G. Király, G. Nagy, A. Lend, Z. Dudás, V. Papp, Z. Balogh, K. Moldován, L. Juhász, C. Cserháti, Z. Szántó, I. Fábián, J. Kalmár, Mechanism of hydration of biocompatible silica-casein aerogels probed by NMR and SANS reveal backbone rigidity, Appl. Surf. Sci. 531 (2020) 147232.
[70] P. Veres, M. Keri, I. Banyai, I. Lazar, I. Fabian, C. Domingo, J. Kalmar, Mechanism of drug release from silica-gelatin aerogel-Relationship between matrix structure and release kinetics, Colloids Surf. B: Biointerfaces 152 (2017) 229–237.
[71] M. Keri, A. Forgacs, V. Papp, I. Banyai, P. Veres, A. Len, Z. Dudas, I. Fabian, J. Kalmar, Gelatin content governs hydration induced structural changes in silica-gelatin hybrid aerogels - Implications in drug delivery, Acta Biomater. 105 (2020) 131–145.
[72] I. Smirnova, S. Suttiruengwong, W. Arlt, Feasibility study of hydrophilic and hydrophobic silica aerogels as drug delivery systems, J. Non-Cryst. Solids 350 (2004) 54–60.
[73] C. Wang, S. Okubayashi, 3D aerogel of cellulose triacetate with supercritical antisolvent process for drug delivery, J. Supercrit. Fluids 148 (2019) 33–41.
[74] P. Veres, A.M. Lopez-Periago, I. Lazar, J. Saurina, C. Domingo, Hybrid aerogel preparations as drug delivery matrices for low water-solubility drugs, Int. J. Pharm. 496 (2015) 360–370.
[75] I. Smirnova, S. Suttiruengwong, W. Arlt, Aerogels: Tailor-made carriers for immediate and prolonged drug release, KONA 23 (2005) 86–96.
[76] A. Bang, A.G. Sadekar, C. Buback, B. Curtin, S. Acar, D. Kolasinac, W. Yin, D. A. Rubenstein, H. Lu, N. Leventis, C. Sotiriou-Leventis, Evaluation of dysprosia aerogels as drug delivery systems: a comparative study with random and ordered mesoporous silicas, ACS Appl. Mater. Interfaces 6 (2014) 4891–4902.
[77] Y. Fu, W.J. Kao, Drug release kinetics and transport mechanisms of non-degradable and degradable polymeric delivery systems, Expert Opin. Drug Deliv. 7 (2010) 429–444.
[78] E. Haimer, M. Wendland, K. Schlufter, K. Frankenfeld, P. Miethe, A. Potthast, T. Rosenau, F. Liebner, Loading of bacterial cellulose aerogels with bioactive compounds by antisolvent precipitation with supercritical carbon dioxide, Macromol. Symp. 294-II (2010) 64–74.
[79] R.W. Korsmeyer, S.R. Lustig, N.A. Peppas, Solute and penetrant diffusion in swellable polymers. I. Mathematical modelling, J. Polym. Sci. Part A-2 Polym. Phys. 24 (1986) 395.
[80] S. Cardea, L. Baldino, E. Reverchon, Comparative study of PVDF-HFP-curcumin porous structures produced by supercritical assisted processes, J. Supercrit. Fluids 133 (2018) 270–277.
[81] M.A. Marin, R.R. Mallepally, M.A. McHugh, Silk fibroin aerogels for drug delivery applications, J. Supercrit. Fluids 91 (2014) 84–89.
[82] A.N. Mustapa, A. Martin, L.M. Sanz-Moral, M. Rueda, M.J. Cocero, Impregnation of medicinal plant phytochemical compounds into silica and alginate aerogels, J. Supercrit. Fluids 116 (2016) 251–263.
[83] J. Siepmann, N.A. Peppas, Higuchi equation: derivation, applications, use and misuse, Int. J. Pharm. 418 (2011) 6–12.
[84] H.B. Hopfenberg, Controlled release from erodible slabs, cylinders, and spheres, in: D.R. Paul, F.W. Harris (Eds.), Controlled Release Polymeric Formulations, ACS Symp. Ser. No. 33, American Chemical Society, Washington, 1976, pp. 26–32.
[85] M. Mohammadian, T.S.J. Kashi, M. Erfan, F.P. Soorbaghi, In-vitro study of ketoprofen release from synthesized silica aerogels (as drug carriers) and evaluation of mathematical kinetic release models, Iran. J. Pharm. Res. 17 (2018) 818–829. PMC6094426.
[86] T. Ukmar, U. Maver, O. Planinšek, V. Kaučič, M. Gaberšček, A. Godec, Understanding controlled drug release from mesoporous silicates: theory and experiment, J. Control. Release 155 (2011) 409–417.
[87] T. Ukmar, U. Maver, O. Planinšek, A. Pintar, V. Kaučič, A. Godec, M. Gaberšček, Guest–host van der Waals interactions decisively affect the molecular transport in mesoporous media, J. Mater. Chem. 22 (2012) 1112–1120.
[88] A. Charalabidis, M. Sfouni, C. Bergstrom, P. Macheras, The Biopharmaceutics Classification System (BCS) and the Biopharmaceutics Drug Disposition Classification System (BDDCS): beyond guidelines, Int. J. Pharm. 566 (2019) 264–281.

[89] S. Hua, Advances in oral drug delivery for regional targeting in the gastrointestinal tract - influence of physiological, pathophysiological and pharmaceutical factors, Front. Pharmacol. 11 (2020) 524.
[90] M. Bermejo, B. Sanchez-Dengra, M. Gonzalez-Alvarez, I. Gonzalez-Alvarez, Oral controlled release dosage forms: dissolution versus diffusion, Expert Opin. Drug Deliv. 17 (2020) 791–803.
[91] J. das Neves, R. Sverdlov Arzi, A. Sosnik, Molecular and cellular cues governing nanomaterials-mucosae interactions: from nanotherapeutics to nanotoxicology, Chem. Soc. Rev. 49 (2020) 5058–5100.
[92] S. Kalepu, V. Nekkanti, Insoluble drug delivery strategies: review of recent advances and business prospects, Acta Pharm. Sin. B 5 (2015) 442–453.
[93] R. Laitinen, K. Löbmann, C.J. Strachan, H. Grohganz, T. Rades, Emerging trends in the stabilization of amorphous drugs, Int. J. Pharm. 453 (2013) 65–79.
[94] E.C.L. Jones, L.M. Bimbo, Crystallisation behaviour of pharmaceutical compounds confined within mesoporous silicon, Pharmaceutics 12 (2020) 214.
[95] S.K. Rajanna, M. Vinjamur, M. Mukhopadhyay, Mechanism for formation of hollow and granular silica aerogel microspheres from rice husk ash for drug delivery, J. Non-Cryst. Solids 429 (2015) 226–231.
[96] S.K. Rajanna, M. Vinjamur, M. Mukhopadhyay, Robust silica aerogel microspheres from rice husk ash to enhance the dissolution rate of poorly water-soluble drugs, Chem. Eng. Commun. 204 (2017) 249–253.
[97] K. Möller, T. Bein, Degradable drug carriers: vanishing mesoporous silica nanoparticles, Chem. Mater. 31 (2019) 4364–4378.
[98] N. Murillo-Cremaes, A.M. Lopez-Periago, J. Saurina, A. Roig, C. Domingo, Nanostructured silica-based drug delivery vehicles for hydrophobic and moisture sensitive drugs, J. Supercrit. Fluids 73 (2013) 34–42.
[99] R.M. Obaidat, M. Alnaief, H. Mashaqbeh, Investigation of carrageenan aerogel microparticles as a potential drug carrier, AAPS PharmSciTech 19 (2018) 2226–2236.
[100] P. Del Gaudio, G. Auriemma, T. Mencherini, G. Della Porta, E. Reverchon, R. P. Aquino, Design of alginate-based aerogel for nonsteroidal anti-inflammatory drugs controlled delivery systems using prilling and supercritical-assisted drying, J. Pharm. Sci. 102 (2013) 185–194.
[101] D. Lovskaya, N. Menshutina, Alginate-based aerogel particles as drug delivery systems: investigation of the supercritical adsorption and in vitro evaluations, Materials 13 (2020) 329.
[102] P. Franco, I. De Marco, Supercritical CO_2 adsorption of non-steroidal anti-inflammatory drugs into biopolymer aerogels, J. CO2 Util. 36 (2020) 40–53.
[103] D.D. Lovskaya, A.E. Lebedev, N.V. Menshutina, Aerogels as drug delivery systems: in vitro and in vivo evaluations, J. Supercrit. Fluids 106 (2015) 115–121.
[104] J. Pawar, M.T. Ali, R. Fule, K. Moravkar, M. Seervi, S. Sathaye, P. Amin, Biodegradable porous starch spheres as a novel carrier for enhancement of dissolution rate and oral bioavailability of itraconazole, Current Drug Deliv. 14 (2017) 944–954.
[105] A. Ubeyitogullari, R. Moreau, D.J. Rose, O.N. Ciftci, In vitro bioaccessibility of low-crystallinity phytosterol nanoparticles generated using nanoporous starch bioaerogels, J. Food Sci. 84 (2019) 1812–1819.
[106] I. De Marco, E. Reverchon, Starch aerogel loaded with poorly water-soluble vitamins through supercritical CO_2 adsorption, Chem. Eng. Res. Des. 119 (2017) 221–230.
[107] J. Salonen, L. Laitinen, A.M. Kaukonen, J. Tuura, M. Björkqvist, T. Heikkilä, K. Vähä-Heikkilä, J. Hirvonen, V.P. Lehto, Mesoporous silicon microparticles for oral drug delivery: loading and release of five model drugs, J. Control. Release 108 (2005) 362–374.
[108] M.B. Lim, A.S. Ganas, J.L. Hanson, X.Z. Zhou, B. Hellner, S. Manandhar, R. E. Gariepy, F. Baneyx, D.S. Wilbur, P.J. Pauzauskie, Crystalline loading of lipophilic Coenzyme Q(10) pharmaceuticals within conjugated carbon aerogel derivatives, Carbon 164 (2020) 451–458.
[109] T. Mehling, I. Smirnova, U. Guenther, R.H.H. Neubert, Polysaccharide-based aerogels as drug carriers, J. Non-Cryst. Solids 355 (2009) 2472–2479.
[110] C.A. García-González, I. Smirnova, Use of supercritical fluid technology for the production of tailor-made aerogel particles for delivery systems, J. Supercrit. Fluids 79 (2013) 152–158.
[111] L. Wang, R.J. Mu, L.Z. Lin, X.H. Chen, S.S. Lin, Q.W. Ye, J. Pang, Bioinspired aerogel based on konjac glucomannan and functionalized carbon nanotube for controlled drug release, Int. J. Biol. Macromol. 133 (2019) 693–701.
[112] G.K. Eleftheriadis, M. Filippousi, V. Tsachouridou, M.A. Darda, L. Sygellou, I. Kontopoulou, N. Bouropoulos, T. Steriotis, G. Charalambopoulou, I. S. Vizirianakis, G. Van Tendeloo, D.G. Fatouros, Evaluation of mesoporous carbon aerogels as carriers of the non-steroidal anti-inflammatory drug ibuprofen, Int. J. Pharm. 515 (2016) 262–270.
[113] J. Bhandari, H. Mishra, P.K. Mishra, R. Wimmer, F.J. Ahmad, S. Talegaonkar, Cellulose nanofiber aerogel as a promising biomaterial for customized oral drug delivery, Int. J. Nanomedicine 12 (2017) 2021–2031.
[114] G. Tkalec, Z. Knez, Z. Novak, pH sensitive mesoporous materials for immediate or controlled release of NSAID, Microporous Mesoporous Mater. 224 (2016) 190–200.
[115] P. Veres, D. Sebok, I. Dekany, P. Gurikov, I. Smirnova, I. Fabian, J. Kalmar, A redox strategy to tailor the release properties of Fe(III)-alginate aerogels for oral drug delivery, Carbohydr. Polym. 188 (2018) 159–167.
[116] G. Tkalec, Z. Knez, Z. Novak, Fast production of high-methoxyl pectin aerogels for enhancing the bioavailability of low-soluble drugs, J. Supercrit. Fluids 106 (2015) 16–22.
[117] G. Horvat, M. Pantic, Z. Knez, Z. Novak, Encapsulation and drug release of poorly water soluble nifedipine from bio-carriers, J. Non-Cryst. Solids 481 (2018) 486–493.
[118] A. Veronovski, G. Tkalec, Z. Knez, Z. Novak, Characterisation of biodegradable pectin aerogels and their potential use as drug carriers, Carbohydr. Polym. 113 (2014) 272–278.
[119] R. Wang, D. Shou, O. Lv, Y. Kong, L.H. Deng, J. Shen, pH-Controlled drug delivery with hybrid aerogel of chitosan, carboxymethyl cellulose and graphene oxide as the carrier, Int. J. Biol. Macromol. 103 (2017) 248–253.
[120] H. Ayazi, O. Akhavan, M. Raoufi, R. Varshochian, N.S.H. Motlagh, F. Atyabi, Graphene aerogel nanoparticles for in-situ loading/pH sensitive releasing anticancer drugs, Colloids Surf. B: Biointerfaces 186 (2020) 110712.
[121] X.X. Wang, J.M. Wang, S.S. Feng, Z.A. Zhang, C. Wu, X.X. Zhang, F.Y. Kang, Nano-porous silica aerogels as promising biomaterials for oral drug delivery of paclitaxel, J. Biomed. Nanotechnol. 15 (2019) 1532–1545.
[122] H.Y. Li, C. Sun, H.L. Liu, X.Q. Bai, J.G. Wang, D.Q. Wei, B.L. Zhang, X.L. Liao, H. M. Li, H. Li, Aerogel fabricated with halloysite nanoclay as ibuprofen and dexamethasone carrier for dual drugs release, Mater. Res. Express 6 (2019) 105333.
[123] L. Shao, Y. Cao, Z. Li, W. Hu, S. Li, L. Lu, Dual responsive aerogel made from thermo/pH sensitive graft copolymer alginate-g-P(NIPAM-co-NHMAM) for drug controlled release, Int. J. Biol. Macromol. 114 (2018) 1338–1344.
[124] X. Zhang, Y. Wang, J. Zhao, M. Xiao, W. Zhang, C. Lu, Mechanically strong and thermally responsive cellulose nanofibers/poly(N-isopropylacrylamide) composite aerogels, ACS Sustain. Chem. Eng. 4 (2016) 4321–4327.
[125] M. Betz, C.A. Garcia-Gonzalez, R.P. Subrahmanyam, I. Smirnova, U. Kulozik, Preparation of novel whey protein-based aerogels as drug carriers for life science applications, J. Supercrit. Fluids 72 (2012) 111–119.
[126] C. Kleemann, R. Schuster, E. Rosenecker, I. Selmer, I. Smirnova, U. Kulozik, In-vitro-digestion and swelling kinetics of whey protein, egg white protein and sodium caseinate aerogels, Food Hydrocoll. 101 (2020) 105534.
[127] S. Giray, T. Bal, A.M. Kartal, S. Kizilel, C. Erkey, Controlled drug delivery through a novel PEG hydrogel encapsulated silica aerogel system, J. Biomed. Mater. Res. A 100A (2012) 1307–1315.
[128] C.A. Bugnone, S. Ronchetti, L. Manna, M. Banchero, An emulsification/internal setting technique for the preparation of coated and uncoated hybrid silica/alginate aerogel beads for controlled drug delivery, J. Supercrit. Fluids 142 (2018) 1–9.
[129] S. Antonyuk, S. Heinrich, P. Gurikov, S. Raman, I. Smirnova, Influence of coating and wetting on the mechanical behaviour of highly porous cylindrical aerogel particles, Powder Technol. 285 (2015) 34–43.
[130] N. Murillo-Cremaes, P. Subra-Paternault, J. Saurina, A. Roig, C. Domingo, Compressed antisolvent process for polymer coating of drug-loaded aerogel nanoparticles and study of the release behavior, Colloid Polym. Sci. 292 (2014) 2475–2484.
[131] E. Tiryaki, Y.B. Elalmis, B.K. Ikizler, S. Yucel, Novel organic/inorganic hybrid nanoparticles as enzyme-triggered drug delivery systems: dextran and dextran aldehyde coated silica aerogels, J. Drug Deliv. Sci. Tech. 56 (2020) 101517.
[132] F. De Cicco, P. Russo, E. Reverchon, C.A. García-González, R.P. Aquino, P. Del Gaudio, Prilling and supercritical drying: A successful duo to produce core-shell polysaccharide aerogel beads for wound healing, Carbohydr. Polym. 147 (2016) 482–489.
[133] K. Rehman, M.H. Zulfakar, Recent advances in gel technologies for topical and transdermal drug delivery, Drug Dev. Ind. Pharm. 40 (2014) 33–440.
[134] E.B. Yahya, F. Jummaat, A.A. Amirul, A.S. Adnan, N.G. Olaiya, C.K. Abdullah, S. Rizal, M.K.M. Haafiz, H.P.S.A. Khalil, A review on revolutionary natural biopolymer-based aerogels for antibacterial delivery, Antibiotics 9 (2020) 648.
[135] M. Afrashi, D. Semnani, Z. Talebi, P. Dehghan, M. Maheronnaghsh, Novel multi-layer silica aerogel/PVA composite for controlled drug delivery, Mater. Res. Express 6 (2019), 095408.
[136] M. Afrashi, D. Semnani, Z. Talebi, P. Dehghan, M. Maheronnaghsh, Comparing the drug loading and release of silica aerogel and PVA nano fibers, J. Non-Cryst. Solids 503–504 (2019) 186–193.
[137] I. Terzic, J. Ivanovic, I. Zizovic, M. Lucic Skoric, N. Milosavljevic, N. Milasinovic, M.K. Krusic, A. novel chitosan gels, Supercritical CO_2 drying and impregnation with thymol, Polym. Eng. Sci. 58 (2018) 2192–2199.
[138] J.R. Jia, C.X. Wang, A facile restructuring of 3D high water absorption aerogels from methoxy polyethylene glycol-polycaprolactone (mPEG-PCL) nanofibers, Mat. Sci. Eng. C-Mater. 94 (2019) 965–975.
[139] C. Mellado, T. Figueroa, R. Baez, R. Castillo, M. Melendrez, B. Schulz, K. Fernandez, Development development of graphene oxide composite aerogel with proanthocyanidins with hemostatic properties as a delivery system, ACS Appl. Mater. Interfaces 10 (2018) 7717–7729.
[140] H.D.M. Follmann, O.N. Oliveira, D. Lazarin-Bidoia, C.V. Nakamura, X.X. Huang, T. Asefa, R. Silva, Multifunctional hybrid aerogels: hyperbranched polymer-trapped mesoporous silica nanoparticles for sustained and prolonged drug release, Nanoscale 10 (2018) 1704–1715.
[141] Y.D. Sun, Supercritical fluid particle design of dpi formulations (Review), Curr. Pharm. Design 21 (2015) 2516–2542.
[142] X.F. Lin, R.K. Kankala, N. Tang, P.Y. Xu, L.Z. Hao, D.Y. Yang, S.B. Wang, Y. S. Zhang, A.Z. Chen, Supercritical fluid-assisted porous microspheres for efficient delivery of insulin and inhalation therapy of diabetes, Adv. Healthcare Mater. 8 (2019) 1800910.
[143] S. Vyas, S. Dhoble, V. Ghodake, V. Patravale, Xyloglucan based mucosal nanovaccine for immunological protection against brucellosis developed by supercritical fluid technology, Int. J. Pharm. X 2 (2020) 100053.
[144] V.S.S. Gonçalves, P. Gurikov, J. Poejo, A.A. Matias, S. Heinrich, C.M.M. Duarte, I. Smirnova, Alginate-based hybrid aerogel microparticles for mucosal drug delivery, Eur. J. Pharm. Biopharm. 107 (2016) 160–170.

[145] R.M. Obaidat, B.M. Tashtoush, M.F. Bayan, R.T. Al Bustami, M. Alnaief, Drying using supercritical fluid technology as a potential method for preparation of chitosan aerogel microparticles, AAPS PharmSciTech 16 (2015) 1235–1244.
[146] M. Alnaief, R.M. Obaidat, M.M. Alsmadi, Preparation of hybrid alginate-chitosan aerogel as potential carriers for pulmonary drug delivery, Polymers 12 (2020) 2223.
[147] Y.Q. Li, K. Liao, S. Lee, A comparative study of antioxidant-loaded carbon nanoparticles as drug delivery vehicles, RSC Adv. 4 (2014) 56992–56997.
[148] B.S.K. Gorle, I. Smirnova, M.A. McHugh, Adsorption and thermal release of highly volatile compounds in silica aerogels, J. Supercrit. Fluids 48 (2009) 85–92.
[149] N. Abhari, A. Madadlou, A. Dini, Structure of starch aerogel as affected by crosslinking and feasibility assessment of the aerogel for an anti-fungal volatile release, Food Chem. 221 (2017) 147–152.
[150] M. Lehtonen, S. Kekäläinen, I. Nikkilä, P. Kilpeläinen, M. Tenkanen, K. S. Mikkonen, Active food packaging through controlled in situ production and release of hexanal, Food Chem. X 5 (2020) 100074.
[151] F. Sabri, J.D. Boughter, D. Gerth, O. Skalli, T.C.N. Phung, G.R.M. Tamula, N. Leventis, Histological evaluation of the biocompatibility of polyurea crosslinked silica aerogel implants in a rat model: A pilot study, PLoS One 7 (2012) e50686.
[152] G. Nagy, G. Kiraly, P. Veres, I. Lazar, I. Fabian, G. Banfalvi, I. Juhasz, J. Kalmar, Controlled release of methotrexate from functionalized silica-gelatin aerogel microparticles applied against tumor cell growth, Int. J. Pharm. 558 (2019) 396–403.
[153] S.J. Trenfield, A. Awad, C.M. Madla, G.B. Hatton, J. Firth, A. Goyanes, S. Gaisford, A.W. Basit, Shaping the future: recent advances of 3D printing in drug delivery and healthcare, Expert Opin. Drug Deliv. 16 (2019) 1081–1094.
[154] V.C.F. Li, C.K. Dunn, Z. Zhang, Y.L. Deng, H.J. Qi, Direct ink write (DIW) 3D printed cellulose nanocrystal aerogel structures, Sci. Rep. 7 (2017) 8018.
[155] N. Ganonyan, N. Benmelech, G. Bar, R. Gvishi, D. Avnir, Entrapment of enzymes in silica aerogels, Mater. Today 33 (2020) 24–35.
[156] M. Türk, C. Erkey, Synthesis of supported nanoparticles in supercritical fluids by supercritical fluid reactive deposition: current state, further perspectives and needs, J. Supercrit. Fluids 134 (2018) 176–183.
[157] G. Tkalec, M. Pantic, Z. Novak, Z. Knez, Supercritical impregnation of drugs and supercritical fluid deposition of metals into aerogels, J. Mater. Sci. 50 (2015) 1–12.
[158] S.E. Bozbag, N.S. Yasar, L.C. Zhang, M. Aindow, C. Erkey, Adsorption of Pt(cod)me2 onto organic aerogels from supercritical solutions for the synthesis of supported platinum nanoparticles, J. Supercrit. Fluids 56 (2011) 105–113.
[159] H. Gunes, Y. Ozbakir, S.B. Barim, H. Yousefzadeh, S.E. Bozbag, C.A. Erkey, A remarkable class of nanocomposites: aerogel supported bimetallic nanoparticles, Front. Mater. 7 (2020) 18.
[160] X. Gao, R.J.A. Esteves, L. Nahar, J. Nowaczyk, I.U. Arachchige, Direct cross-linking of Au/Ag alloy nanoparticles into monolithic aerogels for application in surface-enhanced raman scattering, ACS Appl. Mater. Interfaces 8 (2016) 13076–13085.
[161] Y. Zhang, Q. Liu, C.B. Ma, Q. Wang, M. Yang, Y. Du, Point-of-care assay for drunken driving with Pd@Pt core-shell nanoparticles-decorated ploy(vinyl alcohol) aerogel assisted by portable pressure meter, Theranostics 10 (2020) 5064–5073.
[162] Y.F. Peng, R.Y. Li, X.L. Sun, G.L. Wang, Z.J. Li, Highly sensitive electrochemical detection of circulating tumor DNA in human blood based on urchin-like gold nanocrystal-multiple graphene aerogel and target DNA-induced recycling double amplification strategy, Anal. Chim. Acta 1121 (2020) 17–25.
[163] F. Guo, X. Zheng, C. Liang, Y. Jiang, Z. Xu, Z. Jiao, Y. Liu, H.T. Wang, H. Sun, L. Ma, W. Gao, A. Greiner, S. Agarwal, C. Gao, Millisecond response of shape memory polymer nanocomposite aerogel powered by stretchable graphene framework, ACS Nano 13 (2019) 5549–5558.
[164] S.J. Dong, Y.N. Zhang, J.Y. Wang, R.R. Cui, X.G. Yu, G.H. Zhao, K.L. Lin, A novel multifunctional carbon aerogel-coated platform for osteosarcoma therapy and enhanced bone regeneration, J. Mater. Chem. B 8 (2020) 368–379.
[165] J.Q. Zhao, C.H. Lu, X. He, X.F. Zhang, W. Zhang, X.M. Zhang, Polyethylenimine-grafted cellulose nanofibril aerogels as versatile vehicles for drug delivery, ACS Appl. Mater. Interfaces 7 (2015) 2607–2615.
[166] N. Murillo-Cremaes, P. Lopez-Aranguren, L.F. Vega, J. Saurina, A. Roig, C. Domingo, A novel solventless coating method to graft low-molecular weight polyethyleneimine on silica fine powders, J. Polym. Sci. A Polym. Chem. 52 (2014) 2760–2768.
[167] S. Yetgin, D. Balkose, Calf thymus DNA characterization and its adsorption on different silica surfaces, RSC Adv. 5 (2015) 57950–57959.
[168] M. Fujiwara, F. Yamamoto, K. Okamoto, K. Shiokawa, R. Nomura, Adsorption of duplex DNA on mesoporous silicas: possibility of inclusion of DNA into their mesopores, Anal. Chem. 77 (2005) 8138–8145.
[169] Y. Xue, Y. Guo, M. Yu, M. Wang, P.X. Ma, B. Lei, Monodispersed bioactive glass nanoclusters with ultralarge pores and intrinsic exceptionally high miRNA loading for efficiently enhancing bone regeneration, Adv. Healthcare Mater. 6 (2017) 1700630.
[170] Y.K. Li, D.K. Yang, Y.C. Chen, H.J. Su, J.C. Wu, Y.W. Chen-Yang, A novel three-dimensional aerogel biochip for molecular recognition of nucleotide acids, Acta Biomater. 6 (2010) 1462–1470.
[171] M. Levin, Pharmaceutical process scale-up, 1st ed., Marcel Dekker, New York, 2001.
[172] N.V. Menshutina, D.D. Lovskaya, A.E. Lebedev, E.A. Lebedev, Production of sodium alginate-based aerogel particles using supercritical drying in units with different volumes, Russian, J. Phys. Chem. B 11 (2017) 1296–1305.
[173] V. Baudron, P. Gurikov, I. Smirnova, A continuous approach to the emulsion gelation method for the production of aerogel micro-particle, Colloid Surf. A 566 (2019) 58–69.
[174] I. De Marco, R. Iannone, S. Miranda, S. Riemma, An environmental study on starch aerogel for drug delivery applications: effect of plant scale up, Int. J. Life Cycle Assess. 23 (2018) 1228–1239.
[175] I. De Marco, S. Riemma, R. Iannone, Life cycle assessment of supercritical impregnation: Starch aerogel plus alpha-tocopherol tablets, J. Supercrit. Fluids 143 (2019) 305–312.
[176] P. Veres, G. Király, G. Nagy, I. Lázár, I. Fábián, J. Kalmár, Biocompatible silica-gelatin hybrid aerogels covalently labeled with fluorescein, J. Non-Cryst. Solids 473 (2017) 17–25.
[177] N.S. Sani, N.A.N.N. Malek, K. Jemon, M.R.A. Kadir, H. Hamdan, Preparation and characterization of hydroxyapatite incorporated silica aerogel and its effect on normal human dermal fibroblast cells, J. Sol-Gel Sci. Technol. 90 (2019) 422–433.